資料

改正「化審法」の施行[1)]

青木康展
Yasunobu AOKI
国立環境研究所環境リスク研究センター副センター長，環境・衛生部会関連法規情報委員会委員

「化学物質の審査及び製造等の規制に関する法律」(以下，「化審法」)の目的は，我が国で製造・輸入される化学物質についてその環境残留性，生体への蓄積性や人の健康や環境への有害性を審査し，有害性等の度合いにより製造・輸入等を管理し，規制する法律である．2009年5月に本法律の大改正が行われ，本年4月に完全施行された．以下，今回の改正に至る背景，問題点，改正の主眼点について解説する．

「化学物質の審査及び製造等の規制に関する法律」

1 化審法とは

「化審法」は「化学物質排出把握管理促進法(PRTR法)」とともに，我が国の環境を経由した化学物質曝露に関する管理の根幹となる法律である．図1に化学物質管理の法令の中での位置付けを示すが，取り扱う事項の専門性ゆえに，厚生労働省，経済産業省，環境省の3省が共管している．PRTR法が人の健康や環境への有害性をもつ化学物質の環境への排出量を把握することを目的とするのに対し，化審法の目的は我が国で製造・輸入される化学物質について，その環境残留性，生体への蓄積性や人の健康や環境への有害性を審査し，有害性等の度合いにより製造・輸入等を管理し，規制することであった．

以下に述べるように，化審法はこれまでも化学物質の安全性の考え方のすう勢にあわせて数度にわたり改正されてきたが，2009年5月に大改正が行われ，本年4月に完全施行された．今回の改正の主眼点は，化学物質の有害性(ハザード)に基づく管理手法だけではなく，有害性と曝露の両方を考慮したリスク評価の考え方に基づく化学物質管理の仕組みを作り，環境中に存在する化学物質の安全と安心に対する懸念に対応しようとするものである．

元来，化審法は「人の健康を損なう恐れまたは動植物の生息若しくは生育に支障を及ぼす恐れがある化学物質による環境の汚染を防止するため」「新規の化学物質の製造または輸入に際し事前にその化学物質の性状に関し審査する制度を設け」さらに「化学物質の性状等に応じ，化学物質の製造，輸入，使用等について必要な規制を行なう」ため，1973年に制定された．制定のきっかけは，米ぬか油に混入

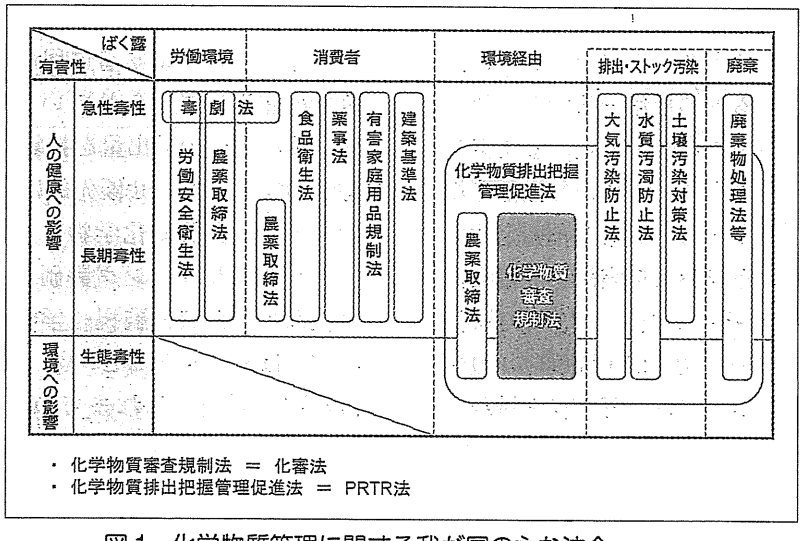

図1 化学物質管理に関する我が国の主な法令
環境省パンフレット「わが国の化学物質対策のこれから」より．

したPCBの摂取を原因とする油症の発生(1968年)である．時を同じくして，環境中(特に沿岸域の底泥)に残留したPCBが食物連鎖を通じて摂取される恐れがあることが国際的にも示され，環境中で分解しにくく(難分解性)，生物に高い濃度で蓄積し(高蓄積性)，かつ人の健康を損なう恐れのある化学物質による環境汚染を防止するための規制が求められた．実は，我が国の化審法は化学物質の管理と規制を目的とした法律として，世界に先駆けて制定されたものである．また，この法律で示された難分解性・高蓄積性の化学物質を優先的に規制・管理する考え方は，現在の国際的な残留性有機汚染物質(persistent organic pollutants；POPs)の規制・管理の枠組みへとつながっている．

化審法の仕組みの特徴は，国内で新たに製造・輸入しようとする化学物質(新規化学物質)を事業者が性状や有害性を試験し，そのデータに基づいて国が審査して，化学物質を分類・指定して管理することにある．1986年および2003年の改正を経て，従前の制度では，難分解性(活性汚泥中での分解性を試験)で，かつ①高蓄積性(魚類(コイ)への蓄積性で試験)の化学物質は第一種監視化学物質，②遺伝毒性やラットへの28日間反復投与の試験結果から人への毒性が疑われる化学物質を第二種監視化学物質，③生態系保全の観点から，生態毒性(魚類(メダカ)，ミジンコ，藻類への毒性)試験結果から動植物への毒性が疑われる化学物質を第三種監視化学物質に指定し，製造と輸入の実績を届けることとしていた．第一種監視化学物質のうち，人または高次捕食動物への長期毒性を有するものを第一種特定化学物質として製造・輸入・使用を事実上禁止，また第二種・第三種監視化学物質のうち，人または生活環境動植物への長期毒性を有するものを第二種特定化学物質として製造・輸入の予定および実績を届け出ることとしていた．しかしその一方，1973年の法律制定以前から使用されていた20,000種類余りの化学物質(既存化学物質)については，国が自ら試験し安全性を点検することとなっていたが，一部またはすべての項目について点検が終了したのは既存化学物質のうち1割弱に過ぎず，大きな問題となっていた．

2 2009年改正の目的：リスク評価に基づく化学物質の管理・規制に向けて

今回の化審法改正の大きな目的の1つは，化学物質に優先順位を付け評価を加速することである．この加速が必要な大きな理由の1つが，化学物質をこれまで以上に安全に使用していこうとする国際的な取り組みである．2002年に開催された「持続可能な開発に関する世界首脳会議(ヨハネスブルグ・サミット；WSSD)」では「予防的取組方法(precautionary approach)に留意しつつ，透明性のある科学的根拠に基づくリスク評価手順と科学的根拠に基づくリスク管理手順を用いて，化学物質が人の健康と環境にもたらす著しい悪影響を最小化する方法で使用，生産されることを2020年までに達成することを目指す」ことが合意され，科学的根拠に基づくリスク評価・管理に向けた取り組みが進んでいる．その典型が2006年に成立した欧州のREACH(registration, evaluation, authorisation and restriction of chemicals，化学物質の登録，評価，認可および制限に関する規則)であり，欧州域内の事業者に製造・輸入するすべての化学物質のリスク評価や，流通経路を通じた化学物質の安全性に関する情報伝達を求めるといった斬新な仕組みが盛り込まれている．各国の取り込みが同時並行で進むなか，我が国でも化審法の審査にリスク評価の考え方を取り入れることとなった．

改正の要点は，①新規化学物質・既存化学物質ともに毎年1トン以上製造・輸入した化学物質の数量と用途について事業者に届出を求めること(従来は毎年の届出は求められていない)，②使用量と用途から環境中への排出量を推算し，人や生態系への有害性の知見とあわせ優先的に安全性評価を行う化学物質を「優先評価化学物質」に指定する(このプロセスをスクリーニング評価という)こと，これに伴い従前の「第二種監視化学物質」「第三種監視化学物質」は廃止すること，③「優先評価化学物質」と「監視化学物質(これまでの第一種監視化学物質)」(後述)については曝露と有害性に関する詳細な情報を収集してリスクを評価し，人または動植物への悪影響が懸念された場合は，「第二種特定化学物質」あるいは「第一種特定化学物質」として製造・使用

表1　改正化審法の下での規制物質の要件

分類	蓄積性・分解性	毒性
第一種特定化学物質	高蓄積性であり難分解性	ヒトへの長期毒性または高次捕食動物への毒性
監視化学物質	高蓄積性であり難分解性	(分解性・蓄積性からのみ判定される)
第二種特定化学物質	高蓄積性ではないが難分解性，あるいは易分解性であってもリスクが十分に低いと認められない場合	ヒトへの長期毒性または生活環境動植物への生態毒性，被害のおそれが認められる環境残留
優先評価化学物質	高蓄積性ではないが難分解性，あるいは易分解性であってもリスクが十分に低いと認められない場合	ヒトへの長期毒性または生活環境動植物への長期毒性の疑い

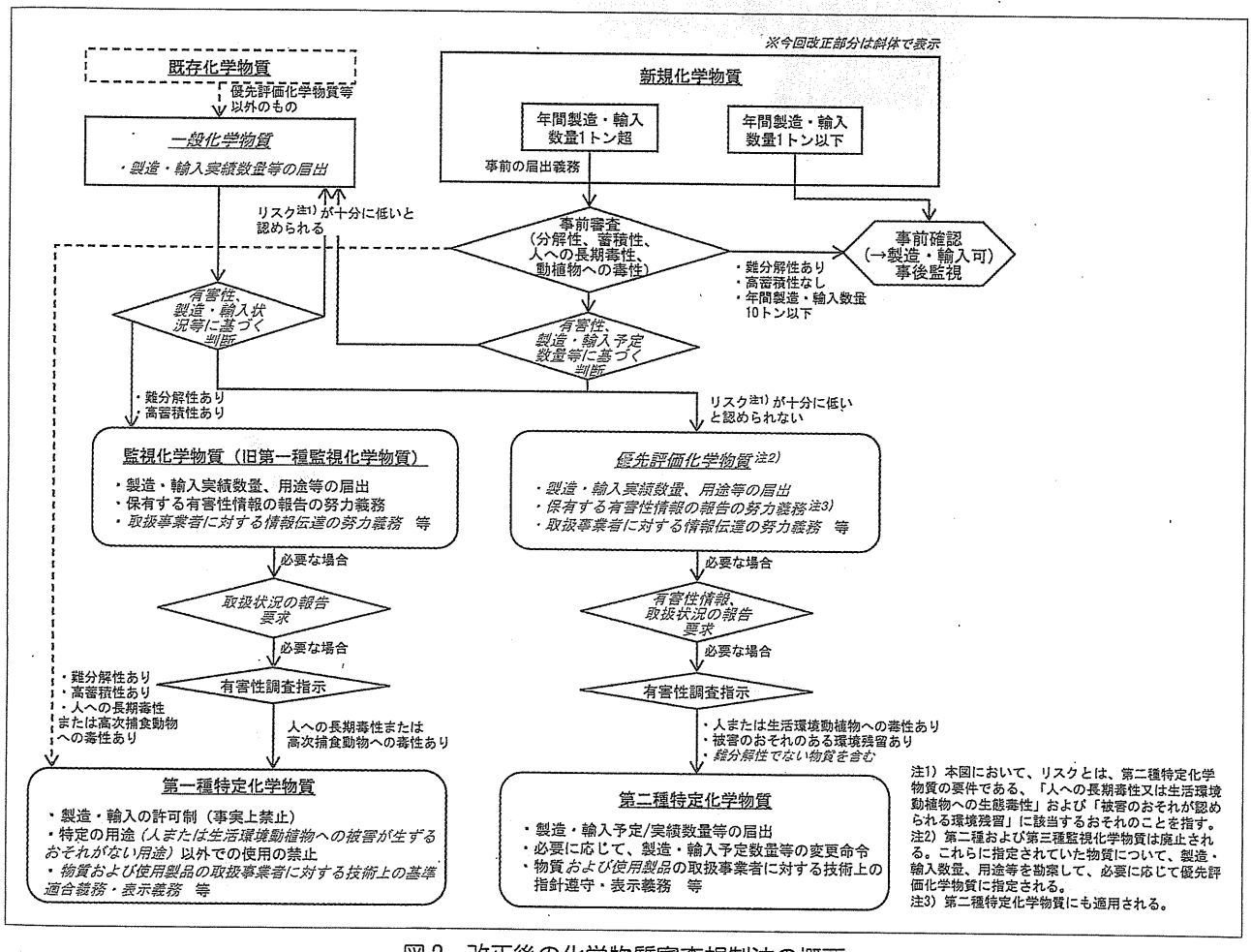

図2　改正後の化学物質審査規制法の概要

環境省HPより改図.

規制の対象とすること，④難分解性でなく「易」分解性の化学物質についても，この法律の対象とし同様に扱うことである．これらの規制の対象となる化学物質の判定基準を，表1にまとめた．

3　改正後の化審法審査の概要

図2に，改正化審法における審査のフローを示す．年間製造・輸入数量が1トン※1を超える新規化学物質については，従前通りの事業者から提出された化学物質の性状や有害性のデータ，製造・輸入予定数量と新たにその用途に基づいて審査する．これまでは，有害性(ハザード)データのみに基づいて化学物質が監視化学物質等に該当するかを判定してい

※1　製造・輸入量が1トン～10トンの化学物質については，原則として難分解性と高蓄積性の審査のみが行われている．

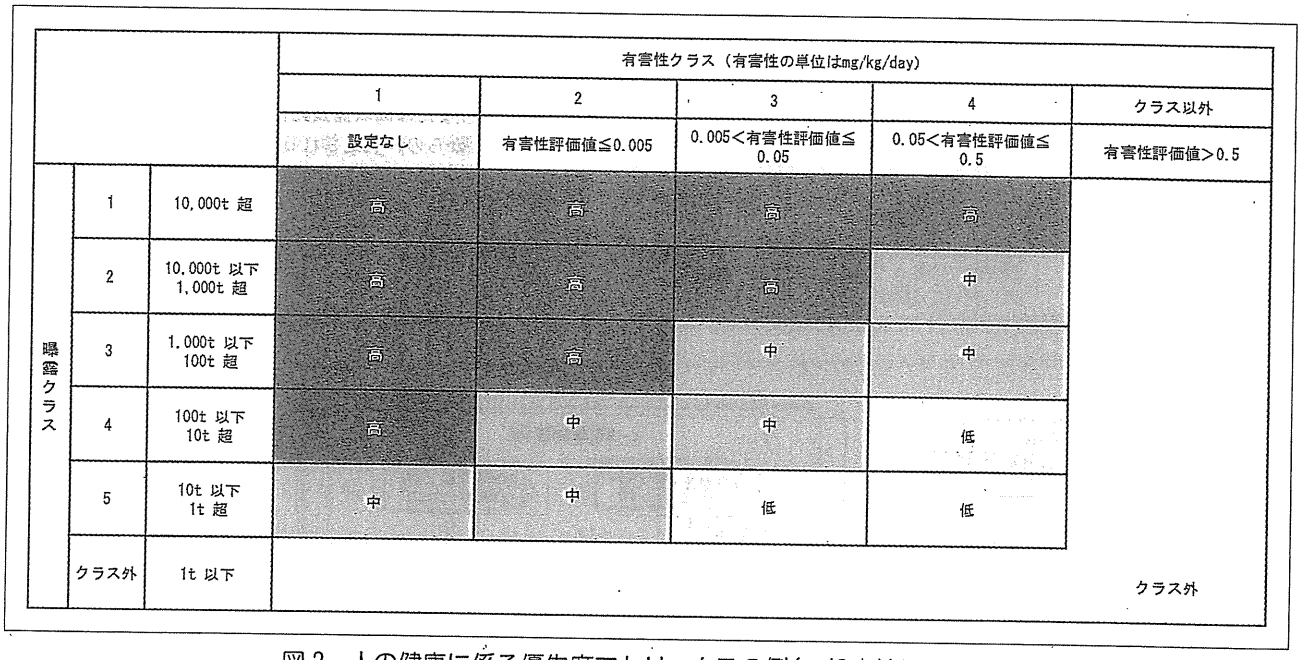

			有害性クラス（有害性の単位はmg/kg/day）				
			1	2	3	4	クラス以外
			設定なし	有害性評価値≦0.005	0.005<有害性評価値≦0.05	0.05<有害性評価値≦0.5	有害性評価値>0.5
曝露クラス	1	10,000t 超	高	高	高	高	
	2	10,000t 以下 1,000t 超	高	高	高	中	
	3	1,000t 以下 100t 超	高	高	中	中	
	4	100t 以下 10t 超	高	中	中	低	
	5	10t 以下 1t 超	中	中	低	低	
	クラス外	1t 以下	クラス外				

図3　人の健康に係る優先度マトリックスの例(一般毒性について)

中央環境審議会資料より改図.

たのに対し，今後は有害性データと大気と水域への排出推定量から審査を行うことになる．この排出推定量とは，用途毎の化学物質の出荷予定量と，デフォルト値として用途毎に設定した排出係数(用途毎に化学物質の大気や水域への排出割合を推定した値)を乗じて算定値をすべての用途について総和した数値であり，これを基に5分類の「曝露クラス」に分類される(図3)．

有害性のうち人健康影響について，これまでは一般毒性の無作用量(Non-observed effect level；NOEL)や遺伝毒性の強さなどを基に判定していたが，今後一般毒性の場合は，NOEL等をデフォルトで設定した不確実係数で除した数値を指標として，有害性を4分類の「有害性クラス」に分類して判定する．新規化学物質の場合はあまりないケースと思われるが，生殖発生毒性，変異原性や発がん性の場合についても，それぞれの判定基準を定めている．※2「曝露クラス」と「有害性クラス」の組み合わせから優先評価化学物質が選ばれる．現状では図3で示す「曝露クラス」と「有害性クラス」のマトリックスで「高」と示した範ちゅうに該当する化学物質，言い換えれば「曝露クラス」＋「有害性クラス」の値が5より小さい化学物質は“リスクが十分に低いと認められない”として優先評価化学物質と判定される．また，マトリックス上「中」「低」に該当された化学物質についても，専門家の判断により優先評価化学物質と判定される可能性もある．生態毒性についても，健康影響と同じ考え方で「曝露クラス」と「有害性クラス」のマトリックスを作り，優先評価化学物質を判定していく．優先評価化学物質と判定されなかった新規化学物質は，下記の一般化学物質に分類されることとなる．

一方，改正により既存化学物質は一般化学物質と名称を変え，新たに製造・輸入量等の届出が求められる．また，一般化学物質が人の健康に及ぼす影響と生態毒性に関する有害性の知見は，国が収集する．これら製造・輸入量と有害性の知見から，新規化学物質同様に一般化学物質についても「曝露クラス」と「有害性クラス」を分類して優先評価化学物質への判定を行う．一般化学物質については信頼できる有害性の知見が得られない事態も想定されるが，一般毒性についてはデフォルトで「有害性クラス：2」と判定して，有害性が高いクラスに分類す

※2　複数の有害性の項目について「有害性あり」と判定された場合は，最も高い有害性クラスの値を採用する．

表2　第一種特定化学物質一覧(環境省HPより)

CAS番号	物質名	過去の用途例
—	ポリ塩化ビフェニル	絶縁油等
—	ポリ塩化ナフタレン(塩素数が3以上のものに限る)	機械油等
118-74-1	ヘキサクロロベンゼン	殺虫剤等原料
309-00-2	1,2,3,4,10,10-ヘキサクロロ-1,4,4a,5,8,8a-ヘキサヒドロ-エキソ-1,4-エンド-5,8-ジメタノナフタレン(別名アルドリン)	殺虫剤
60-57-1	1,2,3,4,10,10-ヘキサクロロ-6,7-エポキシ-1,4,4a,5,6,7,8,8a-オクタヒドロ-エキソ-1,4-エンド-5,8-ジメタノナフタレン(別名ディルドリン)	殺虫剤
72-20-8	1,2,3,4,10,10-ヘキサクロロ-6,7-エポキシ-1,4,4a,5,6,7,8,8a-オクタヒドロ-エンド-1,4-エンド-5,8-ジメタノナフタレン(別名エンドリン)	殺虫剤
50-29-3	1,1,1-トリクロロ-2,2-ビス(4-クロロフェニル)エタン(別名DDT)	殺虫剤
—	1,2,4,5,6,7,8,8-オクタクロロ-2,3,3a,4,7,7a-ヘキサヒドロ-4,7-メタノ-1H-インデン，1,4,5,6,7,8,8-ヘプタクロロ-3a,4,7,7a-テトラヒドロ-4,7-メタノ-1H-インデンおよびこれらの類縁化合物の混合物(別名クロルデンまたはヘプタクロル)	白アリ駆除剤等
56-35-9	ビス(トリブチルスズ)＝オキシド	漁網防汚剤，船底塗料等
—	N,N′-ジトリル-パラ-フェニレンジアミン，N-トリル-N′-キシリル-パラ-フェニレンジアミン，またはN,N′-ジキシリル-パラ-フェニレンジアミン	ゴム老化防止剤，スチレンブタジエンゴム
732-26-3	2,4,6-トリ-ターシャリ-ブチルフェノール	酸化防止剤その他の調製添加剤(潤滑油用または燃料油用のものに限る)，潤滑油
8001-35-2	ポリクロロ-2,2-ジメチル-3-メチリデンビシクロ[2.2.1]ヘプタン(別名トキサフェン)	殺虫剤，殺ダニ剤(農業用および畜産用)
2385-85-5	ドデカクロロペンタシクロ[5.3.0.0(2,6).0(3,9).0(4,8)]デカン(別名マイレックス)	樹脂，ゴム，塗料，紙，織物，電気製品等の難燃剤，殺虫剤・殺蟻剤
115-32-2	2,2,2-トリクロロ-1,1-ビス(4-クロロフェニル)エタノール(別名ケルセンまたはジコホル)	防ダニ剤
87-68-3	ヘキサクロロブタ-1,3-ジエン	溶媒
3846-71-7	2-(2H-1,2,3-ベンゾトリアゾール-2-イル)-4,6-ジ-*tert*-ブチルフェノール	紫外線吸収剤
1763-23-1, 2795-39-3[a], 4021-47-0[a], 29457-72-5[a], 29081-56-9[a], 70225-14-8[a], 56773-42-3[a], 251099-16-8[a]	ペルフルオロ(オクタン-1-スルホン酸)(別名PFOS)またはその塩	撥水撥油剤，界面活性剤
307-35-7	ペルフルオロ(オクタン-1-スルホニル)＝フルオリド(別名PFOSF)	PFOSの原料
608-93-5	ペンタクロロベンゼン	農薬，副生成物
319-84-6	r-1, c-2, t-3, c-4, t-5, t-6-ヘキサクロロシクロヘキサン(別名α-ヘキサクロロシクロヘキサン)	CAS番号58-89-9の副生成物
319-85-7	r-1, t-2, c-3, t-4, c-5, t-6-ヘキサクロロシクロヘキサン(別名β-ヘキサクロロシクロヘキサン)	CAS番号58-89-9の副生成物
58-89-9	r-1, c-2, t-3, c-4, c-5, t-6-ヘキサクロロシクロヘキサン(別名γ-ヘキサクロロシクロヘキサンまたはリンデン)	農薬，殺虫剤
143-50-0	デカクロロペンタシクロ[5.3.0.$0^{2,6}$.$0^{3,9}$.$0^{4,8}$]デカン-5-オン(別名クロルデコン)	農薬，殺虫剤
36355-01-8	ヘキサブロモビフェニル	難燃剤
40088-47-9[b]	テトラブロモ(フェノキシベンゼン)(別名テトラブロモジフェニルエーテル)	難燃剤
32534-81-9[b]	ペンタブロモ(フェノキシベンゼン)(別名ペンタブロモジフェニルエーテル)	難燃剤
68631-49-2[c], 207122-15-4[c]	ヘキサブロモ(フェノキシベンゼン)(別名ヘキサブロモジフェニルエーテル)	難燃剤
446255-22-7[c], 207122-16-5[c]	ヘプタブロモ(フェノキシベンゼン)(別名ヘプタブロモジフェニルエーテル)	難燃剤

a)ペルフルオロオクタンスルホン酸塩の例
b)商業用ペンタブロモジフェニルエーテルに含まれる代表的な異性体
c)商業用オクタブロモジフェニルエーテルに含まれる代表的な異性体
色字は，2010年4月に追加された物質

ることとしている．また，一般化学物質のうち難分解性であり，高蓄積性の化学物質は監視化学物質（これまでの第一種監視化学物質）と判定する．ちなみに今回の改正により，一般化学物質についても毎年の製造・輸入量の届出が求められることから，製造・輸入量が増えることで新たに優先評価化学物質に指定される可能性もある．

優先評価化学物質あるいは監視化学物質と判定された化学物質については，事業者に図2のように届出などの義務が課せられる．また優先評価化学物質や監視化学物質について，必要な場合に，国は事業者に有害性情報や取扱状況の報告を求め，さらに有害性調査を指示し，得られた知見を基にリスク評価を行うこととなるが，このリスク評価の手法の詳細は現在検討中である．リスク評価の結果，人または動植物に毒性があり，あるいは被害の恐れのある環境残留ありと判定されると，第一種特定化学物質や第二種特定化学物質に指定される．この指定により，これらの化学物質には，同じく図2にあるような，より厳しい手法による管理が求められることになる．

4 どのような化学物質が化審法の管理のもとにあるか？

さて，WSSD合意の達成年次である2020年は，実は目の前である．ここ10年のうちに事業者や国の積極的な取り組みにより，これからも増えるであろう新規化学物質と20,000種類を上回る一般化学物質のすべてがリスク評価の対象となり，優先評価化学物質や監視化学物質，さらに第一種特定化学物質や第二種特定化学物質に指定され，その化学物質の使用により想定されるリスクに見合った管理が行われることが期待される．どのような化学物質がこれまでに指定され，今後指定されていくのか大いに興味がある．このうち，最も管理の厳しい第一種特定化学物質に指定されている化学物質を表2に示す．さらに，製品評価技術基盤機構による化審法データベース[2]は最もよい情報源の1つであり，参照されたい．

引用文献

1) 本資料は，環境・衛生部会内に設置された関連法規情報委員会（委員長：姫野誠一郎　徳島文理大学教授）が衛生薬学関連法規の改正等に関する情報を提供するものである．
2) http://www.safe.nite.go.jp/jcheck/Top.do

Book Review
新刊紹介

合成有機化学
反応機構によるアプローチ

R.K.Parashar　著
柴田高範，小笠原正道，鹿又宣弘，
斎藤慎一，庄司　満　訳

東京化学同人／A5・464頁・6,825円

有機合成化学の教科書は，既に定評のあるものが出版されている．また，反応機構に関する良書も少なくない．ところが，両者を兼ね備えたものにはこれまでお目にかかったことはなかった．本書は，その空白を埋める1冊である．代表的な合成反応を反応機構とともに詳しく解説しているため，読者は合成反応の官能基選択性や立体選択性などを反応機構を基礎として理解でき，記憶に残すことができる．

構成は，極めてオーソドックスなものである．1章で逆合成や極性転換，各種選択性の説明，保護基の概念といった総論に続き，2章において反応中間体が詳しく解説されている．3章でアルドール反応等の炭素–炭素単結合の形成反応が，4章でWittig反応を中心とする炭素–炭素二重結合形成反応が，5章で遷移金属触媒を用いるカップリング反応がまとめられ，3〜5章で骨格形成反応の解説を行っている．6章，7章で官能基変換の要である還元と酸化を扱っている．最後の8章では，ペリ環状が軌道の対称性とともに解説されている．本文中には，1，2か所の疑問点はあるものの，訳者が脚注で訂正しているので全く問題ない．翻訳書の長所である．

約400頁のA5判にコンパクトにまとめられており，日本語で読めるので，基礎的知識を素早くチェックするのにまさにうってつけである．有機化学を一通り学んだ修士1年クラスの学生に，安心して勧められる書である．

田村　修　Osamu TAMURA

※本書は，日本薬学会「薬学情報コーナー」で閲覧できます．

DNA Repair 11 (2012) 259–266

Contents lists available at SciVerse ScienceDirect

DNA Repair

journal homepage: www.elsevier.com/locate/dnarepair

Activation of AMP-activated protein kinase by MAPO1 and FLCN induces apoptosis triggered by alkylated base mismatch in DNA

Teik How Lim[a], Ryosuke Fujikane[b], Shiori Sano[b,c], Ryuji Sakagami[c], Yoshimichi Nakatsu[a], Teruhisa Tsuzuki[a], Mutsuo Sekiguchi[d], Masumi Hidaka[b,*]

[a] Department of Medical Biophysics and Radiation Biology, Faculty of Medical Sciences, Kyushu University, Fukuoka 812-8582, Japan
[b] Department of Physiological Science and Molecular Biology, Fukuoka Dental College, Fukuoka 814-0193, Japan
[c] Department of Odontology, Fukuoka Dental College, Fukuoka 814-0193, Japan
[d] Frontier Research Center, Fukuoka Dental College, Fukuoka 814-0193, Japan

ARTICLE INFO

Article history:
Received 31 August 2011
Received in revised form 9 November 2011
Accepted 28 November 2011
Available online 29 December 2011

Keywords:
AMPK
Apoptosis
Folliculin/BHD
MAPO1/FNIP2/FNIPL
O^6-methylguanine

ABSTRACT

O^6-Methylguanine produced in DNA by the action of simple alkylating agents, such as *N*-methyl-*N*-nitrosourea (MNU), causes base-mispairing during DNA replication, thus leading to mutations and cancer. To prevent such outcomes, the cells carrying O^6-methylguanine undergo apoptosis in a mismatch repair protein-dependent manner. We previously identified MAPO1 as one of the components required for the induction of apoptosis triggered by O^6-methylguanine. MAPO1, also known as FNIP2 and FNIPL, forms a complex with AMP-activated protein kinase (AMPK) and folliculin (FLCN), which is encoded by the *BHD* tumor suppressor gene. We describe here the involvement of the AMPK–MAPO1–FLCN complex in the signaling pathway of apoptosis induced by O^6-methylguanine. By the introduction of siRNAs specific for these genes, the transition of cells to a population with sub-G_1 DNA content following MNU treatment was significantly suppressed. After MNU exposure, phosphorylation of AMPKα occurred in an MLH1-dependent manner, and this activation of AMPK was not observed in cells in which the expression of either the *Mapo1* or the *Flcn* gene was downregulated. When cells were treated with AICA-ribose (AICAR), a specific activator of AMPK, activation of AMPK was also observed in a MAPO1- and FLCN-dependent manner, thus leading to cell death which was accompanied by the depolarization of the mitochondrial membrane, a hallmark of the apoptosis induction. It is therefore likely that MAPO1, in its association with FLCN, may regulate the activation of AMPK to control the induction of apoptosis triggered by O^6-methylguanine.

1. Introduction

Most of the DNA lesions produced by internal and external agents can be removed by cellular DNA repair enzymes, while cells with un-repaired lesions are eliminated by apoptosis. The biological significance of these two mechanisms is clearly shown when organisms lacking one or both of these cellular functions are exposed to simple alkylating agents, such as *N*-methyl-*N*-nitrosourea (MNU) and *N*-methyl-*N'*-nitro-*N*-nitrosoguanidine (MNNG), which alkylate purine and pyrimidine bases in DNA [1]. Among the various modified bases thus produced, O^6-methylguanine is of particular importance since this modified base can pair with thymine as well as cytosine during DNA replication, leading to induction of mutation and cancer [2,3]. Organisms possess a specific DNA repair enzyme, O^6-methylguanine–DNA methyltransferase (MGMT), which transfers a methyl-group from O^6-methylguanine in DNA onto the enzyme molecule, thereby repairing the DNA lesion in a single step reaction [4,5]. When the modified base is not repaired, an O^6-methylguanine–thymine pair is formed through DNA replication and this mismatch can be recognized by a mismatch repair protein complex, composed of MSH2, MSH6, MLH1 and PMS2, which induces apoptosis to exclude cells carrying the mutation-evoking DNA lesions [6–8]. It is noteworthy that *Mgmt*$^{-/-}$ mice, which lack the DNA repair enzyme specific for O^6-methylguanine, are hypersensitive to both the killing and to the tumorigenic action of alkylating chemicals [9–12] and these dual effects can be dissociated by the introduction of an additional defect in mismatch repair genes. Mice with mutations in both alleles of the *Mgmt* and the *Mlh1* genes, the latter encoding a protein involved in the recognition of mismatched base, are as resistant to MNU as are wild-type mice in terms of survival, but are much more susceptible to MNU-induced tumorigenesis than wild-type mice

* Corresponding author at: Department of Physiological Science and Molecular Biology, Fukuoka Dental College, 2-15-1 Tamura, Sawara-ku, Fukuoka 814-0193, Japan. Tel.: +81 92 801 0411x310; fax: +81 92 801 0685.
E-mail address: hidaka@college.fdcnet.ac.jp (M. Hidaka).

1568-7864/$ – see front matter © 2011 Elsevier B.V. All rights reserved.
doi:10.1016/j.dnarep.2011.11.006

[13]. Consistent with these results, *Mgmt*$^{-/-}$ *Mlh1*$^{-/-}$ cells, derived from the gene-targeted mice, are unable to induce apoptosis and show an elevated mutant frequency after MNU treatment [14].

The apoptotic signal initiated through the mismatch recognition complex activates a signaling cascade leading to the cell cycle checkpoints and apoptotic pathways for cell death. Both the release of cytochrome C from the mitochondria as well as the activation of Apaf-1 and caspase-3, hallmarks of the induction of apoptosis, have been demonstrated after the treatment of cells with alkylating agents that produce O^6-methylguanine [14,15]. However, the precise molecular mechanism underlying the signal transduction downstream of mismatch recognition still remains to be determined. To identify the factors involved in the O^6-methylguanine-induced apoptotic process, we screened MNU-resistant clones derived from MNU-sensitive *Mgmt*$^{-/-}$ cells using retrovirus-mediated gene-trap mutagenesis [16]. Mouse-derived KH101 cells, carrying an insertional mutation in one of the alleles of an uncharacterized gene, were unable to induce mitochondrial membrane depolarization as well as caspase-3 activation, after treatment with MNU. In this way, we identified a new gene, designated as *Mapo1* (O^6-methylguanine induced apoptosis 1), which was related to the induction of apoptosis. The mutant frequency of KH101 cells was significantly elevated after the treatment with MNU, thus supporting the notion that the induction of apoptosis, in which the MAPO1 is involved, contributes significantly to the elimination of cells carrying mutation-inducing DNA lesions. A search in the database revealed that the amino acid sequence of the MAPO1 protein is homologous to that of folliculin-interacting protein 1 (FNIP1), which was identified as a protein having the capacity to associate with folliculin [17]. Folliculin is a tumor suppressor protein with unknown biological activity, and is encoded by the *FLCN* gene. Mutations in the *FLCN* gene have been found in patients with Birt-Hogg-Dubé (BHD) syndrome [18,19], which is characterized by the development of hair follicle hamartomas, lung cysts, and an increased risk for renal neoplasia [20–22]. Identification of another folliculin-interacting protein, displaying a similarity in its amino acid sequence to that of FNIP1, was reported by two groups of researchers and the gene responsible was named *FNIP2* and *FNIPL*, respectively [23,24]. The *FNIP2/FNIPL* gene turned out to be the same gene as the human homolog of *Mapo1*. It was also reported that FNIP2/FNIPL, as well as FNIP1, could bind to 5′-AMP-activated protein kinase (AMPK), composed of AMPKα, β and γ subunits, which is an important energy sensor in cells that negatively regulates cell growth and proliferation [25,26].

We report here that a complex composed of MAPO1, FLCN and AMPK is involved in the induction of apoptosis triggered by O^6-methylguanine–thymine mispair. Evidence is presented which shows that during the course of apoptosis induction, the phosphorylation of AMPKα occurs in a MAPO1- and FLCN-dependent manner.

2. Materials and methods

2.1. Cell lines and cell culture

The YT102 (*Mgmt*$^{-/-}$ *Mlh1*$^{+/+}$), YT103 (*Mgmt*$^{-/-}$ *Mlh1*$^{-/-}$) and KH101 (*Mgmt*$^{-/-}$ *Mapo1*$^{+/-}$) cell lines were established as described previously [14,16]. The cells were cultivated in Dulbecco's modified Eagle's medium (D-MEM) supplemented with 10% fetal bovine serum (FBS) at 37 °C in 5% CO_2.

2.2. Chemicals

N-Methyl-*N*-nitrosourea (MNU) was obtained from Sigma. Compound C and AICA-Ribose were purchased from Calbiochem.

2.3. Immunoprecipitation and immunoblotting

To prepare cells expressing Flag-tagged MAPO1 or HA-tagged FLCN, a pIRES-puro3 vector (Clontech) containing mouse-derived *Mapo1* cDNA tagged with Flag epitope at the carboxy terminal end or a pIRES-puro2 (Clontech) vector carrying mouse-derived *Flcn* cDNA tagged with the HA epitope at the amino terminal end was introduced into YT102 cells using Lipofectamine 2000 (Invitrogen) according to the manufacturer's protocol. For the immunoprecipitation, the cells were lysed with NETN buffer (50 mM Tris/HCl (pH 8.0), 150 mM NaCl, 0.2% NP-40, 1 mM EDTA) containing protease inhibitors (Roche). To precipitate the Flag-tagged MAPO1, 10 μl of anti-FLAG M2-agarose (Sigma) were added to the extract, and incubated for 4 h at 4 °C. Alternatively, 10 μl of anti-HA (HA-7)-agarose (Sigma) were added to precipitate the HA-tagged FLCN, and the mixture was incubated overnight at 4 °C. After extensive washing of the beads with NETN buffer, the proteins bound to the beads were eluted in 40 μl of 2× SDS-PAGE sample buffer (120 mM Tris/HCl (pH 6.8), 4% SDS, 20% glycerol, 200 mM DTT, 0.002% bromophenol blue).

For the immunoblotting analyses, immunoprecipitated materials or whole cell extracts prepared by the lysis of cells with 2× SDS-PAGE sample buffer were subjected to SDS-PAGE and electroblotted onto a PVDF membrane (Bio-Rad). Detection was performed using an ECL Plus or Advance Western blotting detection kit (GE Healthcare). The primary antibodies used were: anti-FLAG M2 (Sigma), anti-HA HA-7 (Sigma), anti-FLCN (Protein Tech Group, Inc.), anti-AMPKα (Cell signaling), anti-β-actin (Sigma), and anti-phospho-AMPKα (Thr172) (Cell signaling). Anti-mouse IgG and anti-rabbit IgG conjugated to horseradish peroxidase (GE Healthcare) were used as the secondary antibodies.

2.4. siRNA transfection

Stealth RNAi for the *Mapo1* gene (siMapo1), 5′-CAGAAAGCAGAGGAUGUUCCUAUUA-3′, *Flcn* gene (siFlcn#1), 5′-UUAUUCAGGAUAGUGGGCCCAACUC-3′, (siFlcn#2), 5′-UGGUGACUGACGUACUUAAUAGAGG-3′, and *Ampkα* gene (siAmpkα#1), 5′-UAUCUUAGCGUUCAUCUGGGCAUCC-3′, (siAmpkα#2), 5′-AAGAUGAUAAGCCACUGCAAGCUGG-3′ were purchased from Invitrogen. After culturing 1×10^5 cells in a 6-well plate for one day, the cells were transfected with 20 nM siRNA, using the Lipofectamine RNAiMAX reagent (Invitrogen) according to the manufacturer's protocol. For the control transfection, Stealth RNAi Negative Control Medium GC Duplex (Invitrogen) was used.

2.5. Flow cytometric analysis

For the sub-G_1 population assay, cells were washed with PBS and suspended in 400 μl of PBS containing 0.1% Triton X-100, 25 μg/ml of propidium iodide and 0.1 mg/ml of RNase A. The samples were analyzed using a FACS Calibur flow cytometer (Becton Dickinson), with 10,000 events per determination.

For the mitochondrial membrane depolarization assay, cells were treated with the MitoProbeTM DiOC2(3) Assay Kit (Invitrogen), according to the manufacturer's protocol, and then subjected to analysis using a FACS Calibur flow cytometer.

2.6. Trypan blue exclusion assay

The viability of YT102, KH101 and siRNA-transfected YT102 cells was assayed, based on their trypan blue exclusion. The cells treated with AICA-Ribose were collected 48 h after the drug treatment and were stained with 0.2% trypan blue. The percentage of dead cells was determined as the percentage of trypan blue staining-positive cells. At least 500 cells were counted per experiment.

2.7. Statistics

All *P*-values were generated using two-tailed Student's *t*-tests.

3. Results

3.1. Interaction of MAPO1 with FLCN and AMPK

To confirm that MAPO1 protein interacts with FLCN and AMPK, a co-immunoprecipitation experiment was performed. Whole cell extracts were prepared from mouse YT102 (*Mgmt*$^{-/-}$) cells expressing Flag-tagged MAPO1, and were subjected to immunoprecipitation using an anti-Flag antibody conjugated to agarose beads. The results are shown in Fig. 1A. With whole cell extracts, almost the same intensity of bands for FLCN and AMPKα were detected in both control and Flag-MAPO1-transfected cells. When the materials were immunoprecipitated with the anti-Flag antibody, co-precipitated FLCN and AMPKα were clearly detected, concomitant with the effective precipitation of Flag-MAPO1, whereas no such bands were seen in a sample precipitated from cells treated with the control vector alone.

To evaluate the interaction of FLCN with MAPO1 and AMPK in a reciprocal manner, whole cell extracts prepared from YT102 cells expressing FLAG-tagged MAPO1, with or without HA-tagged FLCN, were applied for immunoprecipitation using an anti-HA antibody (Fig. 1B). When the HA-tagged FLCN was precipitated, as indicated by doublet bands by the immunoblotting analysis, the Flag-tagged MAPO1 and AMPKα were co-precipitated. It is evident, therefore, that MAPO1 interacts with FLCN and AMPK in mouse cells.

3.2. Suppression of the induction of apoptosis in Flcn- and Ampkα-knockdown cells

Since MAPO1 has been identified as an apoptosis-inducing protein, it is plausible that the MAPO1-bound proteins, FLCN and AMPK, might also be involved in apoptosis induction. To examine the possible roles of these proteins, siRNAs specific for the *Flcn* or *Ampkα* genes were introduced into YT102 (*Mgmt*$^{-/-}$) cells. As shown in Fig. 2A and B, two independent siRNAs (siFlcn#1 and #2, and siAmpkα#1 and #2), designed at different sequences of each gene, effectively suppressed the expression of the genes when measured at 48 h after their introduction. The expression level of the *Mapo1* gene in siMapo1-treated cells also decreased to 43% of that in cells that were treated with the control RNA, siCont, as measured by quantitative real time PCR [16]. To monitor the appearance of cells with sub-G_1 DNA content, cells were treated with or without 0.4 mM MNU for 1 h and subjected to a flow cytometric analysis 72 h later. After treatment with MNU, the sub-G_1 cell population increased to more than 20% in the siCont-treated cells (Fig. 2C). Under the same conditions, the degrees of the increases in the cells treated with siRNAs against the *Flcn*, *Ampkα* and *Mapo1* genes were significantly suppressed. These results favor the notion that FLCN and AMPKα, as well as MAPO1, are involved in MNU-induced apoptosis through protein interactions.

3.3. Suppression of the induction of apoptosis by an AMPK inhibitor

The effects of *Ampkα* knockdown on the MNU-induced apoptosis were further examined at multiple time points. The YT102 cells transfected with siCont or siAmpkα#2 were exposed to 0.4 mM MNU for 1 h and then subjected to a flow cytmetric analysis. As shown in Fig. 3A, the sub-G_1 cell population increased gradually, with similar kinetics in cells transfected with either type of siRNA, but the degree of the increase in cells transfected with siAmpkα was significantly lower than that of siCont-transfected cells.

To obtain further evidence supporting the involvement of AMPK in MNU-induced apoptosis, compound C, a specific inhibitor of AMPK, was used to downregulate the function of AMPK. YT102 cells were exposed to 0.4 mM MNU for 1 h, followed by incubation with or without 2 μM of compound C for 72 h, and then cells were subjected to a flow cytometric analysis. As shown in Fig. 3B, the sub-G_1 cell population in compound C-treated cells after MNU treatment significantly decreased in comparison to those not treated with the inhibitor. The inhibitory effects of compound C on AMPK activity were assessed by immunoblotting using an antibody that specifically recognizes a phosphorylated form of AMPKα, since AMPK is activated when the catalytic subunit of AMPKα becomes phosphorylated [27–29]. As shown in Fig. 3C, AMPK appeared to be activated after MNU treatment, while such activation was significantly suppressed by the exposure of cells to compound C. These findings are consistent with the notion that AMPK plays an important role in the induction of apoptosis triggered by MNU.

3.4. MAPO1- and FLCN-dependent activation of AMPK during the induction of apoptosis

To further examine if AMPKα is phosphorylated during the induction of apoptosis, YT102 cells were treated with 1 mM MNU and then collected at 0, 24, 48 and 72 h after treatment. Under these conditions, apoptosis was effectively induced, as was evident by the detection of the mitochondrial membrane depolarization and the caspase-3 activity [16]. The whole cell extracts were prepared, and the phosphorylation levels of AMPKα were assessed by

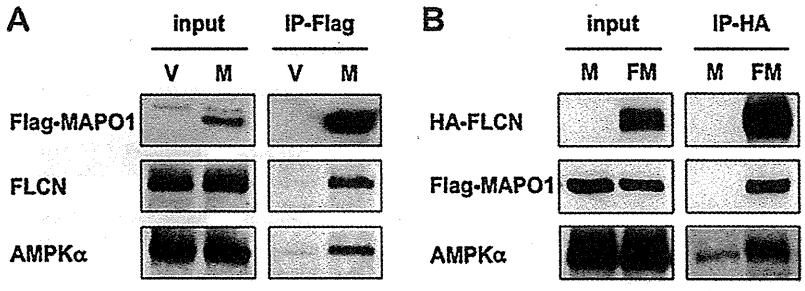

Fig. 1. The association of MAPO1, FLCN and AMPKα proteins. (A) The interaction of MAPO1 with FLCN and AMPKα. YT102 cells were transfected with the pIRES-puro3 vector (termed as V) or pIRES-puro3 containing Flag-tagged *Mapo1* cDNA (termed as M) and harvested after incubation for 24 h. Whole cell extracts (input) were used for immunoprecipitation using anti-Flag M2 antibody beads (IP-Flag). The materials were subjected to SDS-PAGE, transferred to a membrane and immunoblotted using antibodies that recognize the Flag-tag, FLCN and AMPKα. (B) The interaction of FLCN with MAPO1 and AMPKα. YT102 cells were transfected with either pIRES-puro3 containing Flag-tagged *Mapo1* cDNA (termed as M) or pIRE-puro2 carrying HA-tagged *Flcn* cDNA and pIRES-puro3 containing Flag-tagged *Mapo1* cDNA (termed as FM) and were harvested 24 h later. Following immunoprecipitation using anti-HA HA7 antibody beads (IP-HA), an immunoblotting analysis was performed as described in (A) with anti-HA, anti-Flag and anti-AMPKα antibodies.

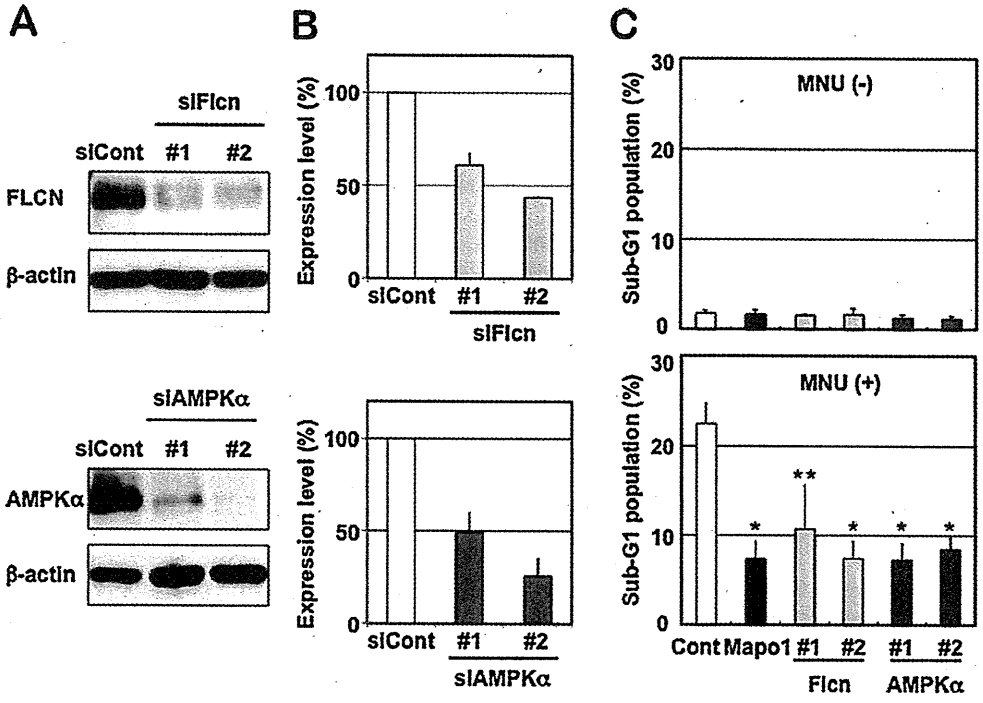

Fig. 2. The suppression of apoptosis by siRNAs targeting the three types of genes. (A) The expression levels of FLCN and AMPKα in cells treated with siRNAs. The whole extracts of YT102 cells transfected with control and two independent siRNAs specific for the corresponding genes were used for the immunoblotting analysis with antibodies specific for FLCN, AMPKα and β-actin (loading control). (B) The relative expression levels of FLCN and AMPKα in the cells treated with siRNAs, as measured by an immunoblotting analysis in (A). (C) The sub-G_1 population of cells transfected with control, *Mapo1*-, *Flcn*- or *Ampkα*-siRNA after MNU treatment. Two days after transfection with siRNA, YT102 cells were treated with or without 0.4 mM MNU for 1 h and then incubated for three days. The cells were harvested and subjected to a flow cytometric analysis. $^*P < 0.01$; $^{**}P < 0.05$ when comparing the sub-G_1 populations in the control and gene-specific siRNA-transfected cells.

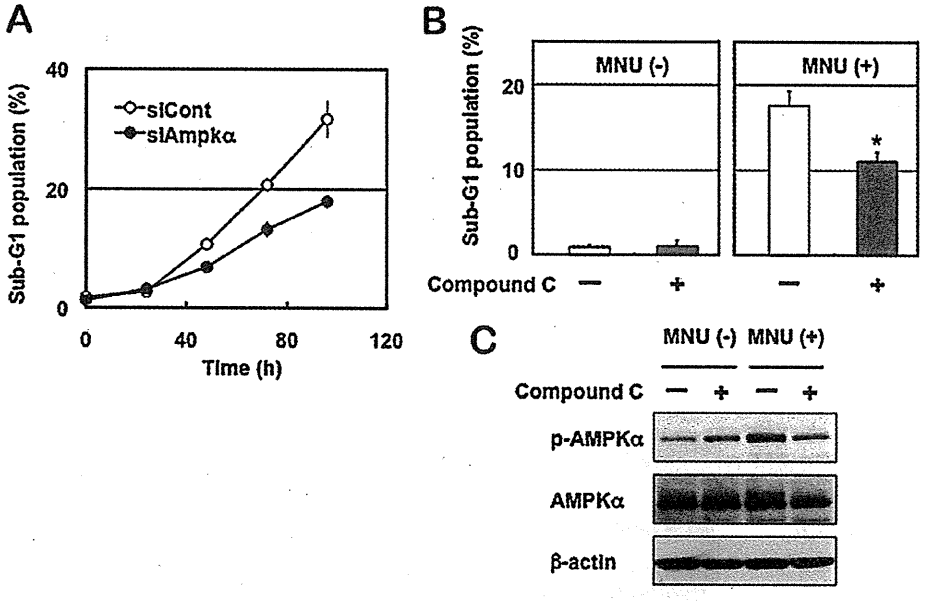

Fig. 3. The involvement of AMPK in MNU-induced apoptosis. (A) The sub-G_1 population of cells transfected with control or *Ampkα* siRNA after MNU treatment. Two days after transfection with siRNA, the YT102 cells were treated with 0.4 mM MNU for 1 h and then harvested at 0, 24, 48, 72 and 96 h after MNU treatment, and subjected to a flow cytometric analysis. The numbers of the cells in the sub-G_1 population were counted and the ratios were plotted. Open circles, siCont-transfected cells; closed circles, siAmpkα-transfected cells. (B) The suppression of apoptosis by an AMPK inhibitor. After treatment with or without 0.4 mM MNU for 1 h, YT102 cells were incubated in medium supplemented with or without 2 μM compound C for three days. The cells were then harvested and subjected to a flow cytometric analysis to monitor the sub-G_1 population of cells. $^*P < 0.01$ when comparing the sub-G_1 populations in compound C-untreated and compound C-treated cells after exposure to MNU. (C) The inhibition of the AMPK activity by compound C. The whole cell extracts from the cells harvested at 48 h after MNU treatment were subjected to an immunoblotting analysis using antibodies that recognize phospho-AMPKα (Thr172), AMPKα and β-actin, respectively.

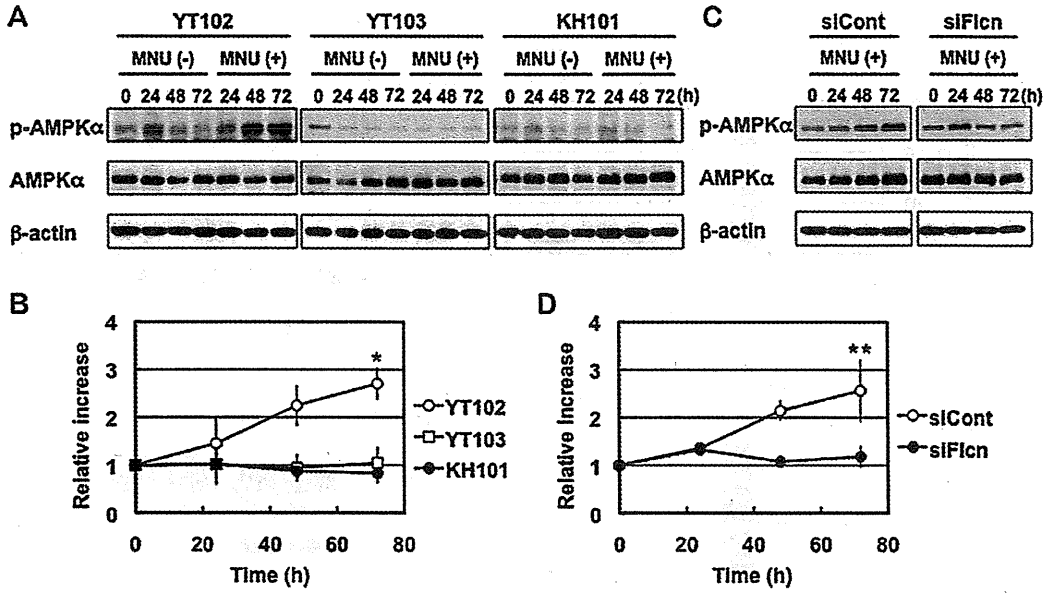

Fig. 4. The activation of AMPK after MNU treatment. (A) The phosphorylation of AMPKα in cells with different genetic backgrounds. Three cell lines, YT102 (*Mgmt*$^{-/-}$), YT103 (*Mgmt*$^{-/-}$ *Mlh1*$^{-/-}$) and KH101 (*Mgmt*$^{-/-}$ *Mapo1*$^{+/-}$), were treated with or without 1 mM MNU for 1 h and then incubated for 0, 24, 48 or 72 h. The whole cell extracts from cells harvested at various times after MNU treatment were subjected to an immunoblotting analysis using antibodies that recognize phospho-AMPKα (Thr172), AMPKα and β-actin, respectively. (B) The relative intensities of the bands for phospho-AMPKα (Thr172) after MNU treatment. Open circles, YT102; open squares, YT103; closed circles, KH101. *$P < 0.01$ when comparing the relative intensities for YT102 cells with those of the YT103 and KH101 cells at 72 h after exposure to MNU. (C) Activation of AMPK in cells transfected with *Flcn*-siRNA. Two days after transfection with control or *Flcn*-siRNA, the YT102 cells were treated with or without 1 mM MNU for 1 h. The analysis was performed as described above. (D) The relative intensities of bands for phospho-AMPKα (Thr172) after MNU treatment. Open circles, siCont-transfected cells; closed circles, siFlcn-transfected cells. **$P < 0.05$ when comparing the relative intensities of the control and *Flcn*-specific siRNA-transfected cells at 72 h after exposure to MNU.

an immunoblotting analysis. As shown in Fig. 4A and B, the levels of phosphorylation of AMPKα increased gradually and reached about 2.7-folds at 72 h after MNU treatment, whereas no such increase was observed in cells not expose to MNU. The amounts of the AMPKα protein were almost constant under these situations. In YT103 (*Mgmt*$^{-/-}$ *Mlh1*$^{-/-}$) cells, which are unable to induce apoptosis due to their lack of the *Mlh1* gene, the increase of phosphorylated forms of AMPKα was hardly detectable, even after MNU treatment. These results indicate that AMPK is activated during the course of the induction of apoptosis, triggered in a mismatch repair protein-dependent manner. To evaluate the effects of *Mapo1* mutation on the activation of AMPK, we used KH101 (*Mgmt*$^{-/-}$ *Mapo1*$^{+/-}$) cells, which carry an insertional mutation in one of the alleles of the *Mapo1* gene and exhibit haploinsufficiency for the induction of apoptosis triggered by MNU treatment [16]. Similar to the results described above, no increase in the band corresponding to phosphorylated AMPKα was detected even after treatment with MNU (Fig. 4A and B). Since MAPO1 interacts with FLCN (Fig. 1), it was supposed that FLCN might also play a role in the activation of AMPK during the course of apoptosis. To examine this possibility, YT102 (*Mgmt*$^{-/-}$) cells were transfected with siRNA targeting the *Flcn* gene (siFlcn#2), and then were exposed to 1 mM MNU for 1 h. The immunoblotting analyses of these samples collected after incubation for 0, 24, 48 and 72 h revealed that phosphorylation of AMPKα, which occurred gradually in siCont-transfected cells, did not take place in the siFlcn-transfected ones (Fig. 4C and D). These results indicate that the activation of AMPK, which occurs during the course of MNU-induced apoptosis, is dependent on the functions of both FLCN and MAPO1.

3.5. Induction of apoptosis through activation of AMPK

To confirm the importance of the activation of AMPK for the induction of apoptosis, AICA-Ribose (AICAR), a specific activator of AMPK, was applied to YT102 cells. After treatment with a low dose (0.2 mM) of AICAR for 48 h, the viabilities of cells were analyzed, based on the trypan blue exclusion assay. As shown in Fig. 5A, there was a significant increase of trypan blue staining-positive cells after treatment with AICAR in the YT102 (*Mgmt*$^{-/-}$ *Mapo1*$^{+/+}$) cells, whereas no such increase was observed in the *Mapo1*-defective KH101 (*Mgmt*$^{-/-}$ *Mapo1*$^{+/-}$) cells even after the same treatment. To determine if the increase in dead cells was related to the induction of apoptosis, the cells were subjected to an assay for mitochondrial membrane depolarization, which is known to occur during the process of apoptosis. The results are shown in Fig. 5B and C. The depolarization of the mitochondrial membrane was induced after treatment with AICAR in YT102 cells, but not in *Mapo1*-defective KH101 cells. The results indicate that the function of MAPO1 is necessary for AICAR-induced apoptosis. An immunoblotting experiment, the results of which are shown in Fig. 5D, revealed that the AICAR-treatment induced phosphorylation of AMPKα to the similar level to that when treated with MNU, however, such an induction did not occur in the *Mapo1*-defective KH101 cells. These results suggest that the activation of AMPK is important for the induction of apoptosis, and that a normal level of MAPO1 is necessary for the activation of AMPK.

We next examined if FLCN, which interacts with MAPO1, is also required for the AICAR-induced cell death. For this study, we applied AICAR to YT102 cells whose FLCN function was knocked down by siRNA (siFlcn#2). As shown in Fig. 6A–C, the degree of AICAR-induced cell death, which was accompanied by the depolarization of the mitochondrial membrane, was significantly lower in siFlcn-transfected cells as compared to that in siCont-transfected ones. Furthermore, the AICAR-induced AMPKα phosphorylation was almost completely blocked in siFlcn-transfected cells (Fig. 6D). Therefore, these results suggest that FLCN is required for AMPK activation, as well as the cell death induced by the treatment with AICAR.

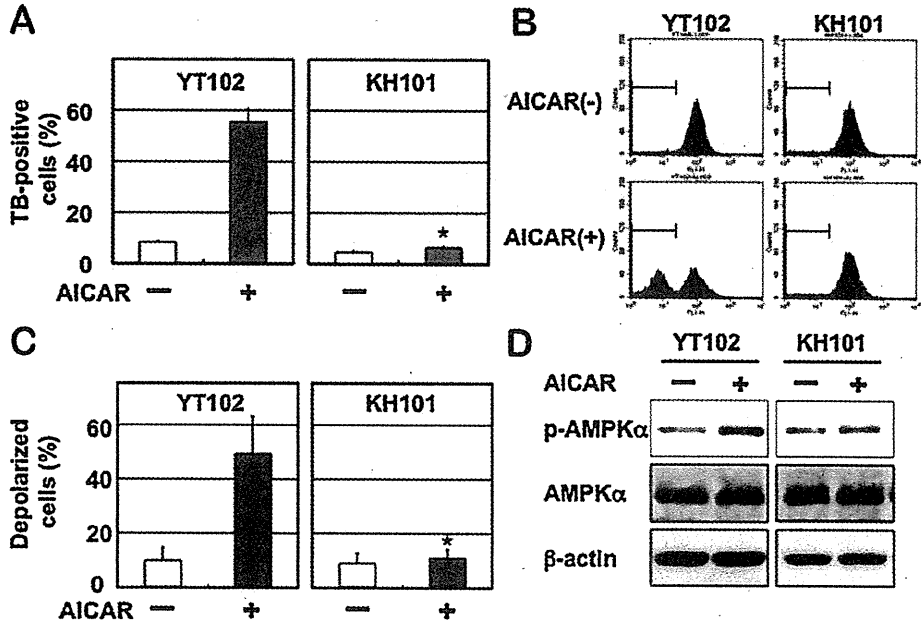

Fig. 5. MAPO1-dependent cell death induced by an AMPK activator. *Mapo1*-proficient YT102 and *Mapo1*-defective KH101 cells were incubated in a medium supplemented with or without 0.2 mM AICAR for two days and then harvested. (A) The viabilities of the cells. The numbers of cells stained with trypan blue (TB) were counted and the ratios are shown. *$P < 0.01$ when comparing the TB-positive YT102 and KH101 cells after exposure to AICAR. (B) Depolarization of the mitochondrial membrane. The cells were evaluated by a mitochondrial membrane depolarization assay, and representative patterns of the assay are shown. The populations of depolarized cells were gated by bars. (C) The levels of mitochondrial membrane depolarization. The mean values obtained from three independent experiments in (B) and the standard deviations (bars) are presented. *$P < 0.01$ when comparing the depolarized cells in YT102 and KH101 cells after exposure to AICAR. (D) Activation of AMPK after treatment with AICAR. The whole cell extracts prepared from cells, treated with or without AICAR, were subjected to an immunoblotting analysis using antibodies specific for phospho-AMPKα (Thr172), AMPKα and β-actin, respectively.

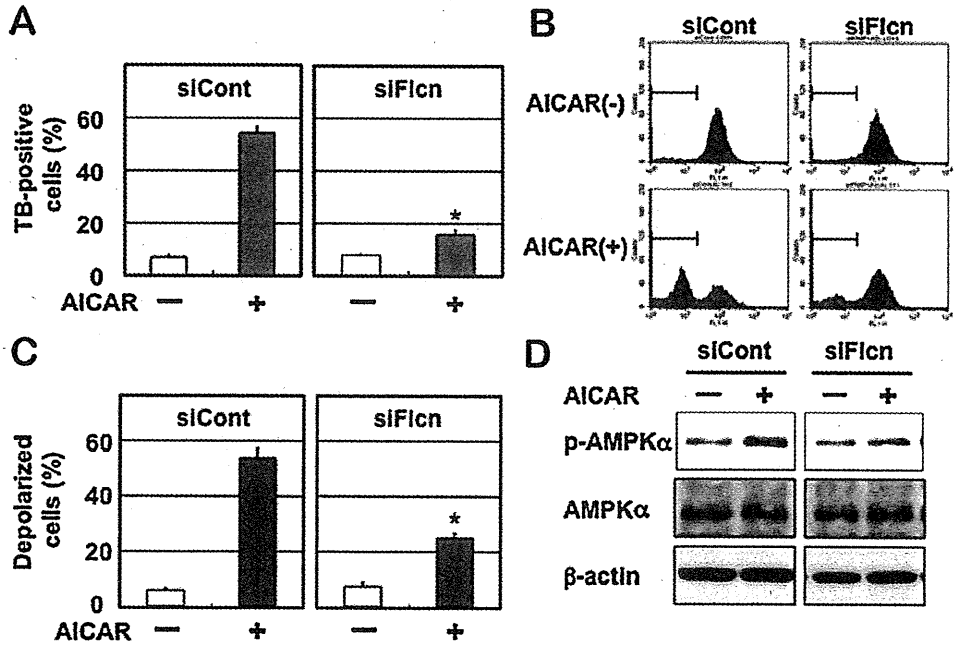

Fig. 6. FLCN-dependent cell death induced by an AMPK activator. YT102 cells transfected with control- or *Flcn*-siRNA were cultured with or without 0.2 mM AICAR for two days and then harvested. (A) The viabilities of the cells. The numbers of cells stained with trypan blue (TB) were counted and the ratios are shown. *$P < 0.01$ when comparing the TB-positive siCont-transfected and siFlcn-transfected cells after exposure to AICAR. (B) Depolarization of the mitochondrial membrane. The cells were evaluated by a mitochondrial membrane depolarization assay, and representative patterns of the assay are shown. The populations of depolarized cells were gated by bars. (C) The levels of mitochondrial membrane depolarization. The mean values obtained from three independent experiments in (B) and the standard deviations (bars) are presented. *$P < 0.01$ when comparing the depolarized cells in siCont-transfected and siFlcn-transfected cells after exposure to AICAR. (D) Activation of AMPK after treatment with AICAR. The whole cell extracts prepared from AICAR-treated or -untreated cells, were subjected to an immunoblotting analysis using antibodies specific for phospho-AMPKα (Thr172), AMPKα and β-actin, respectively.

4. Discussion

MAPO1 was identified as one of the protein elements functioning at a certain step following the induction of apoptosis [16]. In *Mapo1*-defective cells, mitochondrial membrane depolarization and caspase-3 activation were not observed even after exposure to MNU, although the cells retain the ability for mismatch repair protein-dependent DNA damage detection and signaling. Subsequent studies have revealed that MAPO1 is identical to FNIP2 and FNIPL, reported by Hasumi et al. [23] and Takagi et al. [24], respectively. This protein is bound to folliculin, encoded by the *FLCN* tumor suppressor gene, and AMP-activated protein kinase (AMPK). To analyze the possible roles of folliculin and AMPK in the induction of apoptosis, we introduced siRNAs specific for the *Flcn* or *Ampkα* gene and then treated the cells with MNU. The flow cytometric analyses performed to measure the sub-G_1 population of cells revealed that folliculin and AMPK, as well as MAPO1, were involved in MNU-induced apoptosis. Taken together, these data suggest that MAPO1 forms a protein complex(es) with folliculin and AMPK, and plays a role in a signal transduction pathway of apoptosis.

It is known that AMPK is one of the signaling kinases that negatively regulates cell growth and proliferation and is phosphorylated itself under conditions of energetic stress [26–29]. Several recent papers have observed the pro-apoptotic potential of activated AMPK [30–33]. In this report, we found a gradual increase in the levels of AMPK phosphorylation in *Mapo1*-proficient cells after MNU treatment, implying a possible involvement of the activation of AMPK in the MNU-induced apoptosis pathway. In *Mapo1*-deficient cells, AMPK activation in this manner was hardly detectable, even after the treatment with MNU. Furthermore, the treatment of cells with AICAR, a specific activator of AMPK, resulted in AMPKα phosphorylation and mitochondrial membrane depolarization in a *Mapo1*-dependent manner. These findings extended onto the case of *Flcn*-knockdown cells. Taken together, it is likely that MAPO1 and FLCN positively regulate the activation of AMPK through their mutual interaction in the apoptotic signaling pathway, triggered by an alkylating agent. MAPO1 and FLCN proteins have been reported to undergo some modifications in cells [17,24]. The treatment with an alkylating agent might affect the modified states of these proteins, and might cause the activation of the protein complex, thus leading to AMPK activation. Another folliculin-interacting protein, FNIP1, which is homologous to MAPO1, is also capable of binding to AMPK [17]. The activation of AMPK might therefore be regulated in more complex ways under the balance of MAPO1 and FNIP1 activities.

Another important problem which remains to be solved is how the AMPK–MAPO1–FLCN complex is activated by the signal delivered from the mismatch repair protein complex, which itself is activated through the interaction with DNA carrying base mismatches. The signal may be delivered by direct physical contact between the two complexes or through the involvement of other protein factors. The protein linking analyses, aided by mass spectrometry, have been performed, but no evidence to show the physical association of the two complexes was obtained (unpublished results). It seems likely, therefore, that some other protein factor(s) might be involved in the signal transduction process. To identify such factors, it would be relevant to extend this approach using retrovirus-mediated gene-trap mutagenesis studies.

Germline mutations in the *FLCN* gene have been identified in patients with Birt-Hogg-Dubé (BHD) syndrome, which is an autosomal dominant disorder characterized by hamartomas of skin follicles, spontaneous pneumothorax, and renal tumors [20–22]. Furthermore, *BHD* heterozygous knockout mice were revealed to develop kidney cysts and tumors as they aged, while *BHD* homozygous null mice displayed early embryonic lethality [34,35]. The recent findings, including this report, strongly suggest that folliculin has physical and/or functional interactions with the AMPK-mTOR signaling pathway [17,34,36]. Mutations in several other tumor suppressor genes, such as *LKB1*, *TSC1* and *TSC2* [29,37], have also been shown to lead to dysregulation of AMPK-mTOR signaling and to the development of other hamartomatous syndromes. Our present findings that folliculin is involved in the induction of apoptosis might shed some light on the physiological roles of *BHD/FLCN* and other related tumor suppressor genes. We are currently establishing *Mapo1* knockout mice to analyze the possible roles of the gene in the suppression of tumor predisposition resulting from environmental stresses.

Conflict of interest statement

The authors declare that there are no conflicts of interests.

Acknowledgments

We thank Drs. H. Hayakawa and Y. Takagi (Fukuoka Dental College, Japan) for helpful discussion. This work was supported by grants (including a Frontier Research Grant) from the Ministry of Education, Culture, Sports, Science and Technology of Japan, and from the Ministry of Health, Labor and Welfare of Japan.

References

[1] D.T. Beranek, Distribution of methyl and ethyl adducts following alkylation with monofunctional alkylating agents, Mutat. Res. 231 (1990) 11–30.
[2] C. Coulondre, J.H. Miller, Genetic studies of the lac repressor. IV. Mutagenic specificity in the lacI gene of *Escherichia coli*, J. Mol. Biol. 117 (1977) 577–606.
[3] T. Ito, T. Nakamura, H. Maki, M. Sekiguchi, Roles of transcription and repair in alkylation mutagenesis, Mutat. Res. 314 (1994) 273–285.
[4] B. Demple, A. Jacobsson, M. Olsson, P. Robins, T. Lindahl, Repair of alkylated DNA in *Escherichia coli*. Physical properties of O6-methylguanine–DNA methyltransferase, J. Biol. Chem. 257 (1982) 13776–13780.
[5] H. Kawate, K. Ihara, K. Kohda, K. Sakumi, M. Sekiguchi, Mouse methyltransferase for repair of O6-methylguanine and O4-methylthymine in DNA, Carcinogenesis 16 (1995) 1595–1602.
[6] P. Branch, G. Aquilina, M. Bignami, P. Karran, Defective mismatch binding and a mutator phenotype in cells tolerant to DNA damage, Nature 362 (1993) 652–654.
[7] M. Hidaka, Y. Takagi, T.Y. Takano, M. Sekiguchi, PCNA-MutSalpha-mediated binding of MutLalpha to replicative DNA with mismatched bases to induce apoptosis in human cells, Nucleic Acids Res. 33 (2005) 5703–5712.
[8] A. Kat, W.G. Thilly, W.H. Fang, M.J. Longley, G.M. Li, P. Modrich, An alkylation-tolerant, mutator human cell line is deficient in strand-specific mismatch repair, Proc. Natl. Acad. Sci. U.S.A. 90 (1993) 6424–6428.
[9] B.J. Glassner, G. Weeda, J.M. Allan, J.L. Broekhof, N.H. Carls, I. Donker, B.P. Engelward, R.J. Hampson, R. Hersmus, M.J. Hickman, R.B. Roth, H.B. Warren, M.M. Wu, J.H. Hoeijmakers, L.D. Samson, DNA repair methyltransferase (Mgmt) knockout mice are sensitive to the lethal effects of chemotherapeutic alkylating agents, Mutagenesis 14 (1999) 339–347.
[10] K. Sakumi, A. Shiraishi, S. Shimizu, T. Tsuzuki, T. Ishikawa, M. Sekiguchi, Methylnitrosourea-induced tumorigenesis in MGMT gene knockout mice, Cancer Res. 57 (1997) 2415–2418.
[11] A. Shiraishi, K. Sakumi, M. Sekiguchi, Increased susceptibility to chemotherapeutic alkylating agents of mice deficient in DNA repair methyltransferase, Carcinogenesis 21 (2000) 1879–1883.
[12] T. Tsuzuki, K. Sakumi, A. Shiraishi, H. Kawate, H. Igarashi, T. Iwakuma, Y. Tominaga, S. Zhang, S. Shimizu, T. Ishikawa, et al., Targeted disruption of the DNA repair methyltransferase gene renders mice hypersensitive to alkylating agent, Carcinogenesis 17 (1996) 1215–1220.
[13] H. Kawate, K. Sakumi, T. Tsuzuki, Y. Nakatsuru, T. Ishikawa, S. Takahashi, H. Takano, T. Noda, M. Sekiguchi, Separation of killing and tumorigenic effects of an alkylating agent in mice defective in two of the DNA repair genes, Proc. Natl. Acad. Sci. U.S.A. 95 (1998) 5116–5120.
[14] Y. Takagi, M. Takahashi, M. Sanada, R. Ito, M. Yamaizumi, M. Sekiguchi, Roles of MGMT and MLH1 proteins in alkylation-induced apoptosis and mutagenesis, DNA Repair (Amst.) 2 (2003) 1135–1146.
[15] K. Ochs, B. Kaina, Apoptosis induced by DNA damage O6-methylguanine is Bcl-2 and caspase-9/3 regulated and Fas/Caspase-8 independent, Cancer Res. 60 (2000) 5815–5824.
[16] K. Komori, Y. Takagi, M. Sanada, T.H. Lim, Y. Nakatsu, T. Tsuzuki, M. Sekiguchi, M. Hidaka, A novel protein, MAPO1, that functions in apoptosis triggered by O6-methylguanine mispair in DNA, Oncogene 28 (2009) 1142–1150.
[17] M. Baba, S.B. Hong, N. Sharma, M.B. Warren, M.L. Nickerson, A. Iwamatsu, D. Esposito, W.K. Gillette, R.F. Hopkins 3rd, J.L. Hartley, M. Furihata, S. Oishi, W. Zhen, T.R. Burke, W.M. Linehan Jr., L.S. Schmidt, B. Zbar, Folliculin encoded

by the BHD gene interacts with a binding protein, FNIP1, and AMPK and is involved in AMPK and mTOR signaling, Proc. Natl. Acad. Sci. U.S.A. 103 (2006) 15552–15557.
[18] M.L. Nickerson, M.B. Warren, J.R. Toro, V. Matrosova, G. Glenn, M.L. Turner, P. Duray, M. Merino, P. Choyke, C.P. Pavlovich, N. Sharma, M. Walther, D. Munroe, R. Hill, E. Maher, C. Greenberg, M.I. Lerman, W.M. Linehan, B. Zbar, L.S. Schmidt, Mutations in a novel gene lead to kidney tumors, lung wall defects, and benign tumors of the hair follicle in patients with the Birt-Hogg-Dube syndrome, Cancer Cell 2 (2002) 157–164.
[19] C.D. Vocke, Y. Yang, C.P. Pavlovich, L.S. Schmidt, M.L. Nickerson, C.A. Torres-Cabala, M.J. Merino, M.M. Walther, B. Zbar, W.M. Linehan, High frequency of somatic frameshift BHD gene mutations in Birt-Hogg-Dube-associated renal tumors, J. Natl. Cancer Inst. 97 (2005) 931–935.
[20] A.R. Birt, G.R. Hogg, W.J. Dube, Hereditary multiple fibrofolliculomas with trichodiscomas and acrochordons, Arch. Dermatol. 113 (1977) 1674–1677.
[21] J.R. Toro, G. Glenn, P. Duray, T. Darling, G. Weirich, B. Zbar, M. Linehan, M.L. Turner, Birt-Hogg-Dube syndrome: a novel marker of kidney neoplasia, Arch. Dermatol. 135 (1999) 1195–1202.
[22] B. Zbar, W.G. Alvord, G. Glenn, M. Turner, C.P. Pavlovich, L. Schmidt, M. Walther, P. Choyke, G. Weirich, S.M. Hewitt, P. Duray, F. Gabril, C. Greenberg, M.J. Merino, J. Toro, W.M. Linehan, Risk of renal and colonic neoplasms and spontaneous pneumothorax in the Birt-Hogg-Dube syndrome, Cancer Epidemiol. Biomarkers Prev. 11 (2002) 393–400.
[23] H. Hasumi, M. Baba, S.B. Hong, Y. Hasumi, Y. Huang, M. Yao, V.A. Valera, W.M. Linehan, L.S. Schmidt, Identification and characterization of a novel folliculin-interacting protein FNIP2, Gene 415 (2008) 60–67.
[24] Y. Takagi, T. Kobayashi, M. Shiono, L. Wang, X. Piao, G. Sun, D. Zhang, M. Abe, Y. Hagiwara, K. Takahashi, O. Hino, Interaction of folliculin (Birt-Hogg-Dube gene product) with a novel Fnip1-like (FnipL/Fnip2) protein, Oncogene 27 (2008) 5339–5347.
[25] D. Carling, The AMP-activated protein kinase cascade – a unifying system for energy control, Trends Biochem. Sci. 29 (2004) 18–24.
[26] D.G. Hardie, The AMP-activated protein kinase pathway – new players upstream and downstream, J. Cell Sci. 117 (2004) 5479–5487.
[27] S.A. Hawley, M. Davison, A. Woods, S.P. Davies, R.K. Beri, D. Carling, D.G. Hardie, Characterization of the AMP-activated protein kinase from rat liver and identification of threonine 172 as the major site at which it phosphorylates AMP-activated protein kinase, J. Biol. Chem. 271 (1996) 27879–27887.
[28] J.M. Lizcano, O. Goransson, R. Toth, M. Deak, N.A. Morrice, J. Boudeau, S.A. Hawley, L. Udd, T.P. Makela, D.G. Hardie, D.R. Alessi, LKB1 is a master kinase that activates 13 kinases of the AMPK subfamily, including MARK/PAR-1, EMBO J. 23 (2004) 833–843.
[29] R.J. Shaw, M. Kosmatka, N. Bardeesy, R.L. Hurley, L.A. Witters, R.A. DePinho, L.C. Cantley, The tumor suppressor LKB1 kinase directly activates AMP-activated kinase and regulates apoptosis in response to energy stress, Proc. Natl. Acad. Sci. U.S.A. 101 (2004) 3329–3335.
[30] C. Cao, S. Lu, R. Kivlin, B. Wallin, E. Card, A. Bagdasarian, T. Tamakloe, W.M. Chu, K.L. Guan, Y. Wan, AMP-activated protein kinase contributes to UV- and H2O2-induced apoptosis in human skin keratinocytes, J. Biol. Chem. 283 (2008) 28897–28908.
[31] R.G. Jones, D.R. Plas, S. Kubek, M. Buzzai, J. Mu, Y. Xu, M.J. Birnbaum, C.B. Thompson, AMP-activated protein kinase induces a p53-dependent metabolic checkpoint, Mol. Cell 18 (2005) 283–293.
[32] R. Okoshi, T. Ozaki, H. Yamamoto, K. Ando, N. Koida, S. Ono, T. Koda, T. Kamijo, A. Nakagawara, H. Kizaki, Activation of AMP-activated protein kinase induces p53-dependent apoptotic cell death in response to energetic stress, J. Biol. Chem. 283 (2008) 3979–3987.
[33] W.B. Zhang, Z. Wang, F. Shu, Y.H. Jin, H.Y. Liu, Q.J. Wang, Y. Yang, Activation of AMP-activated protein kinase by temozolomide contributes to apoptosis in glioblastoma cells via p53 activation and mTORC1 inhibition, J. Biol. Chem. 285 (2010) 40461–40471.
[34] T.R. Hartman, E. Nicolas, A. Klein-Szanto, T. Al-Saleem, T.P. Cash, M.C. Simon, E.P. Henske, The role of the Birt-Hogg-Dube protein in mTOR activation and renal tumorigenesis, Oncogene 28 (2009) 1594–1604.
[35] Y. Hasumi, M. Baba, R. Ajima, H. Hasumi, V.A. Valera, M.E. Klein, D.C. Haines, M.J. Merino, S.B. Hong, T.P. Yamaguchi, L.S. Schmidt, W.M. Linehan, Homozygous loss of BHD causes early embryonic lethality and kidney tumor development with activation of mTORC1 and mTORC2, Proc. Natl. Acad. Sci. U.S.A. 106 (2009) 18722–18727.
[36] X. Piao, T. Kobayashi, L. Wang, M. Shiono, Y. Takagi, G. Sun, M. Abe, Y. Hagiwara, D. Zhang, K. Okimoto, M. Kouchi, I. Matsumoto, O. Hino, Regulation of folliculin (the BHD gene product) phosphorylation by Tsc2-mTOR pathway, Biochem. Biophys. Res. Commun. 389 (2009) 16–21.
[37] K. Inoki, M.N. Corradetti, K.L. Guan, Dysregulation of the TSC-mTOR pathway in human disease, Nat. Genet. 37 (2005) 19–24.

OXIDATIVE STRESS-INDUCED TUMORIGENESIS IN THE SMALL INTESTINES OF DNA REPAIR-DEFICIENT MICE

Teruhisa Tsuzuki,* Jing Shu Piao,* Takuro Isoda,* Kunihiko Sakumi,† Yusaku Nakabeppu,† and Yoshimichi Nakatsu*

Oxygen radicals are produced through normal cellular metabolism, and the formation of such radicals is further enhanced by radiation and by various chemicals. Oxygen radicals attack DNA and its precursor nucleotides, and consequently bases with various modifications are introduced into the DNA of normally growing cells. One such modified base, 8-oxo-7, 8-dihydroguanine (8-oxoG) is highly mutagenic because of its ambiguous pairing property. Three enzymes, MTH1, OGG1, and MUTYH[1], play important roles in avoiding 8-oxoG-related mutagenesis in mammalian cells (Sekiguchi and Tsuzuki 2002; Sakumi et al. 2003; Tsuzuki et al. 2001, 2007).

The authors have established an experimental system for oxidative DNA damage-induced mutagenesis and tumorigenesis in the gastrointestinal tracts of mice (Sakamoto et al. 2007). Oral administration of an oxidizing reagent, potassium bromate ($KBrO_3$), effectively induced G:C to T:A transversions and epithelial tumors in the small intestines of *Mutyh*-deficient mice, implying the significance of Mutyh in the suppression of mutagenesis and tumorigenesis induced by oxidative stress. Mutation analyses were performed on the tumor-associated genes amplified from the intestinal tumors developed in four mutant mice that had been treated with $KBrO_3$. Many tumors had G:C to T:A transversions in either *Apc* or *Ctnnb1*. No mutations were found in either *K-ras* (exon 2) or *Trp53* (exon 5-8). These findings confirm the association between MUTYH-deficiency and the recessive form of hereditary multiple colorectal adenoma/carcinoma in humans, known as MUTYH-associated familial adenomatous polyposis (Al-Tassan et al. 2002), with the characteristic feature: G:C to T:A transversions in the GAA sequence context. Also, these results suggest that the abnormality in the Wnt signal transduction pathway is causatively associated with oxidative stress-induced tumorigenesis in the small intestines of *Mutyh*-deficient mice. In addition, the multiple formation of tumors in the small intestines of *Mutyh*-deficient mice provides a suitable model system to investigate the processes of intestinal tumorigenesis.[2]

Xie et al. showed that *Mutyh/Ogg1* double-deficient mice predominantly developed lung and ovarian tumors as well as lymphomas (Xie et al. 2004). They also showed that 8.6% of *Mutyh/Ogg1* double-deficient mice exhibited adenomas/carcinomas in their gastrointestinal tracts, which were not observed in wild-type mice. The current researchers and other groups have previously reported that there was little difference in the number of intestinal tumors in wild-type and Ogg1-null mice, although an Ogg1 deficiency resulted in 8-oxoG buildup in genomic DNA and an elevated mutation frequency in the latter (Klungland et al. 1999; Minowa et al. 2000; Sakumi et al. 2003). Thus, the development of intestinal tumors in *Mutyh/Ogg1* double-deficient mice supports the notion that having a Mutyh deficiency does indeed increase susceptibility to intestinal tumorigenesis regardless of the genetic background or environmental factors.

It is of interest that the deficiency of Mutyh but not Ogg1 makes mice susceptible to intestinal tumorigenesis, although the deficiency of either Mutyh or Ogg1 increases G:C to T:A transversion at almost equal frequency in the small intestines of mice. It is possible that this difference may be attributed to the additional substrate; MUTYH excises 2-hydroxyadenine, an oxidized adenine, paired with guanine, beside adenine paired with 8-oxoguanine, from DNA (Ohtusbo et al. 2000; Ushijima et al. 2005). However, Oka et al. recently reported the involvement of Mutyh in cell death caused by oxidative

[1]MUTYH - human protein in print, or gene in italic; Mutyh - mouse counterparts, respectively.

* Department of Medical Biophysics and Radiation Biology, Faculty of Medical Sciences; † Division of Neurofunctional Genomics, Medical Institute of Bioregulation, Kyushu University, Fukuoka, 812-8582 Japan.
For correspondence contact: T. Tsuzuki, Department of Medical Biophysics and Radiation Biology, Faculty of Medical Sciences, Kyushu University, Fukuoka, 812-8582 Japan, or email at tsuzuki@med.kyushu-u.ac.jp.

(*Manuscript accepted* 2 *June* 2010)
0017-9078/10/0

DOI: 10.1097/HP.0b013e3181eaf2c7

[2]Isoda et al., in preparation.

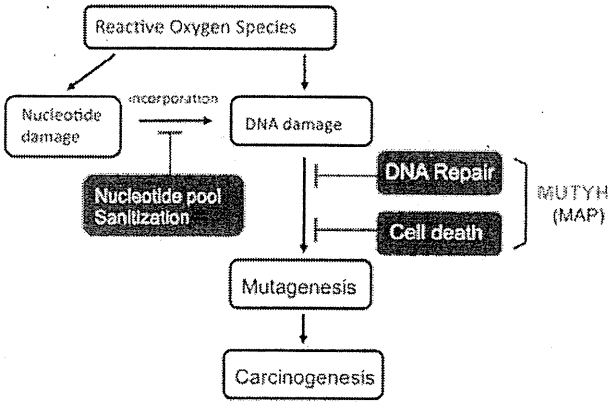

Fig. 1. The roles of MUTYH in the avoiding mechanisms for ROS-induced mutagenesis and carcinogenesis. The defect in Mutyh simultaneously compromises both DNA repair and cell-death induced by oxidative DNA damage. Thus, the defect in Mutyh makes mice highly susceptible to oxidative stress-induced tumorigenesis. This may provide molecular bases for explaining why among the factors involved in suppressing oxidative damage-induced mutagenesis, only MUTYH is, so far, identified to be associated with hereditary colorectal cancers in humans.

DNA damage (Oka et al. 2008). Thus, the defect in Mutyh would simultaneously compromise both DNA repair and cell-death induced by oxidative DNA damage (Fig. 1). This may explain why among the factors involved in suppressing oxidative damage-induced mutagenesis only MUTYH is, so far, identified to be associated with hereditary colorectal cancers in humans.

Acknowledgments—A part of this text is adopted from Extended Abstracts for the 40th International Symposium of the Princess Takamatsu Cancer Research Fund: DNA Repair and Human Cancers, held in November 10–12, 2009, Tokyo, Japan. Health Phys. 100(3):293–294; 2011

Key words: carcinogenesis; mice; radiation, biology; tumors

REFERENCES

Al-Tassan N, Chmiel NH, Maynard J, Fleming N, Livingston AL, Williams GT, Hodges AK, Davies DR, David SS, Sampson JR, Cheadle JP. Inherited variants of MYH associated with somatic G:C to T:A mutations in colorectal tumors. Nat Genet 30:227–232; 2002.

Klungland A, Rosewell I, Hollenbach S, Larsen E, Daly G, Epe B, Seeberg E, Lindahl T, Barnes DE. Accumulation of premutagenic DNA lesions in mice defective in removal of oxidative base damage. Proc Natl Acad Sci USA 96:13300–13305; 1999.

Minowa O, Arai T, Hirano M, Monden Y, Nakai S, Fukuda M, Itoh M, Takano H, Hippou Y, Aburatani H, Masumura K, Nohmi T, Nishimura S, Noda T. *Mmh/Ogg1* gene inactivation results in accumulation of 8-hydroxyguanine in mice. Proc Natl Acad Sci USA 97:4156–4161; 2000.

Ohtsubo T, Nishioka K, Imaiso Y, Iwai S, Shimokawa H, Oda H, Fujiwara T, Nakabeppu Y. Identification of human MutY homolog (hMYH) as a repair enzyme for 2-hydroxyadenine in DNA and detection of multiple forms of hMYH located in nuclei and mitochondria. Nucleic Acids Res 28:1355–1364; 2000.

Oka S, Ohno M, Tsuchimoto D, Sakumi K, Furuichi M, Nakabeppu Y. Two distinct pathways of cell death triggered by oxidative damage to nuclear and mitochondrial DNAs. EMBO J 27:421–432; 2008.

Sakamoto K, Tominaga Y, Yamauchi K, Nakatsu Y, Sakumi K, Yoshiyama K, Egashira A, Kura S, Yao T, Tsuneyoshi M, Maki H, Nakabeppu Y, Tsuzuki T. MUTYH-null mice are susceptible to spontaneous and oxidative stress-induced intestinal tumorigenesis. Cancer Res 67:6599–6604; 2007.

Sakumi K, Tominaga Y, Furuichi M, Xu P, Tsuzuki T, Sekiguchi M, Nakabeppu Y. OGG1 knockout-associated lung tumorigenesis and its suppression by Mth1 gene disruption. Cancer Res 63:902–905; 2003.

Sekiguchi M, Tsuzuki T. Oxidative nucleotide damage: consequences and prevention. Oncogene 21:8895–8904; 2002.

Tsuzuki T, Egashira A, Igarashi H, Iwakuma T, Nakatsuru Y, Tominaga Y, Kawate H, Nakao K, Nakamura K, Ide F, Kura S, Nakabeppu Y, Katsuki M, Ishikawa T, Sekiguchi M. Spontaneous tumorigenesis in mice defective in the MTH1 gene encoding 8-oxo-dGTPase. Proc Natl Acad Sci USA 98:11456–1146; 2001.

Tsuzuki T, Nakatsu Y, Nakabeppu Y. Significance of error-avoiding mechanisms for oxidative DNA damage in carcinogenesis. Cancer Sci 98:465–470; 2007.

Ushijima Y, Tominaga Y, Miura T, Tsuchimoto D, Sakumi K, Nakabeppu Y. A functional analysis of the DNA glycosylase activity of mouse MUTYH protein excising 2-hydroxyadenine opposite guanine in DNA. Nucleic Acids Res 33(2):672–682; 2005.

Xie Y, Yang H, Cunanan C, Okamoto K, Shibata D, Pan J, Barnes DE, Lindahl T, McIlhatton M, Fishel R, Miller JH. Deficiencies in mouse *MYH* and *OGG1* result in tumor predisposition and G to T mutations in codon 12 of the K-ras oncogene in lung tumors. Cancer Res 64:3096–3092; 2004.

Genes and Environment, Vol. 34, No. 1 pp. 18–24 (2012)

Regular article

Evaluation of the Genotoxicity of Aristolochic Acid in the Kidney and Liver of F344 *gpt* delta Transgenic Rat Using a 28-Day Repeated-dose Protocol: A Collaborative Study of the *gpt* delta Transgenic Rat Mutation Assay

Yuji Kawamura[1,6], Hiroyuki Hayashi[2], Osamu Tajima[3], Sayuri Yamada[3], Tomomi Takayanagi[4], Hisako Hori[4], Wataru Fujii[4], Kenichi Masumura[5] and Takehiko Nohmi[5]

[1]Toxicology Laboratory, Pharmaceutical Research Center, Meiji Seika Pharma Co., Ltd., Yokohama, Japan
[2]Research Planning & Management, R&D Planning & Management Dept., Meiji Seika Pharma Co., Ltd., Tokyo, Japan
[3]Food Safety Assurance Center, Quality Assurance & Environment Management Department, Kirin Group Office Co., Ltd.,Yokohama, Japan
[4]Safety Science Institute, Quality Assurance Division, Suntory Business Expert Ltd., Osaka, Japan
[5]Division of Genetics and Mutagenesis, National Institute of Health Sciences, Tokyo, Japan

(Received May 9, 2011; Revised June 20, 2011; Accepted July 5, 2011)

Transgenic rat gene-mutation assays can be used to assess genotoxicity of chemicals in target organs for carcinogenicity. Since gene mutations in transgenes are genetically neutral and thus accumulate along with treatment periods, the assays are suitable for genotoxicity risk assessment of chemicals using repeated-dose treatment methodologies. However, few studies have been conducted to examine the suitability of the assays in repeat-dose treatment protocols. In order to prove the utility of the transgenic rat assays, we treated *gpt* delta rats with aristolochic acid at 0.3 and 1 mg/kg by gavage daily for 28 days, and autopsied the rats 3 days after the final treatment, which is a protocol recommended by the International Workshop on Genotoxicity Testing (IWGT). Aristolochic acid exists in herbs and some other plants, and is carcinogenic in the kidney, bladder and stomach in rats. The mutant frequency (MF) in both the kidney and the liver increased significantly in a dose-dependent manner when the rats were treated with aristolochic acid. We concluded that the *gpt* delta rat assay is sensitive enough to detect gene mutations induced by aristolochic acid and also that the 28-day repeated-dose protocol is suitable for assessing genotoxicity of chemicals.

Key words: F344 *gpt* delta transgenic rat, aristolochic acid, 28-day repeated-dose protocol, *gpt* assay

Introduction

Transgenic gene-mutation assays are of a high value for the assessment of *in vivo* genotoxicity (1,2). In this method, mutations in reporter genes integrated in the rodent chromosomes can be identified in any organs/tissues after the reporter genes are recovered from the rodent cells to bacterial cells. Transgenic gene-mutation assays are suitable for the risk assessment of potential genotoxic chemicals dosed via repeated-dose treatment, since mutations can be analyzed in various time points during treatment and sampling periods (3). In addition, mutations in the reporter genes accumulate over time as the treatments progress (4,5). It is, therefore, expected that these assays enableus to assess the genotoxicity of chemicals with various dose levels, dosing periods and target organs.

Present issues to be solved for the use of transgenic gene-mutation assays include how the detection sensitivity can be confirmed and how the dosing periods can be standardized. In a genotoxicity assessment of 90 carcinogens, transgenic gene-mutation models are shown to have a high sensitivity and a good positive predictability (4). However, the majority of the 90 carcinogens assessed in that study are such strong mutagens that they could be used as positive controls in genotoxicity studies, and there are not enough data available on genotoxicants with a lower potency that allow assess-

[6]Correspondence to: Yuji Kawamura, Toxicology Laboratory, Pharmaceutical Research Center, Meiji Seika Pharma Co., Ltd., 760 Morooka-cho, Kohoku-ku, Yokohama 222-8567, Japan. Tel: +81-45-545-3175, Fax: +81-45-545-3152, E-mail: yuuji.kawamura@meiji.com

ment of the method's sensitivity.

A recent trend regarding the use of experimental animals in toxicological studies focuses on replacement, reduction, and refinement (the '3R' principles), and a movement towards these '3Rs' can be noted in presently reviewed guidelines for the assessment of genotoxicity. In addition to an *in vivo* bone marrow micronucleus test, we may select one more *in vivo* study instead of an *in vitro* study using cultured cells (6), the latter of which shows a comparatively high false-positive rate (7). It is now under discussion and, if conditions permit, we may integrate the *in vivo* genotoxicity assessment into a 28-day repeated-dose toxicity study for example. This approach would contribute to a reduction in the number of animals to be used experimentally. One of the promising candidates for the additional *in vivo* test is a test using a transgenic gene-mutation assay (8). However, nearly 70% of studies with transgenic gene-mutation assays have been conducted using a single dosing or repeated-dosing regimen within a 5-day period (3), and there are not enough data compiled for genotoxicity assessment using repeated treatment. This is contrast to the recommended protocol by the International Workshop on Genotoxicity Testing (IWGT), i.e., autopsy and sample collection on day 3 after the completion of a 28-day repeated treatment (28 + 3 protocol) (9,10,11).

We initiated this study with the aim of testing the adequacy and detection capabilities of the IWGT-recommended general protocol for 28-day repeated-dose studies. For this work, we used F344 *gpt* delta rats, which were developed in Japan (8,12). Aristolochic acid, which exists in herbs and some other plants (13), was used as the test substance, since it is genotoxic *in vitro* and *in vivo* (14,15,16) and carcinogenic in rats (17). In the carcinogenicity in rats, repeated treatment over 6–9 months induced tumors in the kidney, bladder, and stomach (17). In *in vivo* genotoxicity studies in Big Blue transgenic rats (18,19), aristolochic acid was dosed orally for 12 weeks at the same doses used in the carcinogenicity study (17) and the frequency of *cII* mutation in the kidney (18,19), a target organ for carcinogenicity, and the liver, a non-target organ, increased substantially.

In the current study, oral treatments with aristolochic acid increased *gpt* mutant frequency (MF) significantly in the kidney and the liver of F344 *gpt* delta rats in a dose-dependent manner, which suggests that four weeks treatment recommended by IWGT is sensitive enough to detect gene mutations.

Materials and Methods

F344 *gpt* delta rats: All animals were bred at Japan SLC, Inc. (Shizuoka, Japan). The F344 *gpt* delta transgenic rat strain was developed by backcrosses of the original SD *gpt* delta transgenic rat wtih wild-type F344 rats. The *gpt* delta rat contains approximately 5 to 10 copies of the lambda EG10 transgene in chromosome 4 as a heterozygote (12). Male SD *gpt* delta rats were mated with wild-type F344 females to produce heterozygous F1 rats. F1 males (heterozygote for the transgene) were then backcrossed with F344 females. After 15 backcross matings, animals were designated as F344 *gpt* delta rats.

Chemical: Aristolochic acid (CAS#313-67-7, purity 98%, as 8-methoxy-6-nitrophenanthro-(3,4-D)-1,3-dioxolo-5-carboxylic acid, aristolochic acid-I) was purchased from Sigma-Aldrich (Tokyo, Japan). *N*-Ethyl-*N*-nitrosourea (ENU, CAS#759-73-9) was purchased from Nacalai Tesque, Inc. (Kyoto, Japan). The dosing solution of aristolochic acid was prepared by dissolving the chemical in purified water. The dosing solution of ENU was prepared by dissolving the chemical in saline.

Animals and treatments: The rats were used in the experiment at 7 weeks of age, after a 1-week acclimation period. The rats were housed individually in stainless steel cages, with free access to tap water and a CRF-1 pellet diet (Oriental Yeast Co., Ltd., Tokyo, Japan). The animal room conditions were maintained at a room temperature of 23 ± 2°C, a relative humidity of 55 ± 10%, and a light-dark cycle of 12:12 h. The study protocol was approved by the Animal Care and Utilization Committee of Meiji Seika Pharma Co., Ltd. The treatments were conducted in accordance with the protocol recommended by the IWGT (9,10,11). Five *gpt* delta rats per group were dosed with aristolochic acid at 0, 0.3, or 1 mg/kg by gavage daily for 28 days, and necropsied 3 days after the final treatment for collection of the kidney and liver. The following parameters were monitored: clinical signs, body weight, food intake, hematology, blood chemistry, autopsy findings, organ weights, and histopathology. In addition, a positive control group was given an i.p. injection of 50 mg/kg ENU daily for 5 days, and autopsied 26 days after the final treatment for collection of the liver. The collected organs were immediately frozen in liquid nitrogen and stored at −80°C. The frozen samples were sent to Kirin Group Office Co., Ltd. (Lab. A) and Suntory Business Expert Ltd. (Lab. B) for *gpt* assays.

Detection of *gpt* mutation: The *gpt* assays were conducted in accordance with previously published methods in Lab. A and Lab. B separately (1,20). Genomic DNA was extracted from the liver or the kidney using the RecoverEase™ DNA Isolation Kit (Agilent Technologies, Santa Clara, CA) and lambda EG10 phages were recovered with Transpack® Lambda Packaging Extract (Agilent Technologies). *Escherichia coli* YG6020 was infected with the phage, spread onto M9 salt plates containing chloramphenicol (Cm) and 6-thioguanine (6-TG) (21), and then incubated for 72 h at 37°C for selection of the colonies harboring a plasmid

carrying a chloramphenicol acetyltransferase gene and a mutated *gpt* gene. The mutant frequencies (MFs) of the *gpt* gene in the liver and kidney were calculated by dividing the number of confirmed 6-TG resistant colonies by the number of rescued plasmids.

Statistical analysis: The data for MFs were expressed as mean ± SD. Statistically significant differences in MFs between the treated groups and the negative control were analyzed by Dunnett's multiple test or Steel's test. Statistically significant differences in MFs between the positive and negative control groups were analyzed by Welch's t-test. Differences in body weight, food intake, hematology, blood chemistry, and organ weights between the control and treated groups were analyzed by Dunnett's multiple test.

Results

***gpt* Mutations in the liver and kidney induced by aristolochic acid:** In order to estimate the mutagenicity of aristolochic acid, *gpt* delta rats were treated orally for 28 days and mutations in the liver and kidney were analyzed in Lab. A and Lab. B (Fig. 1). Two laborato-

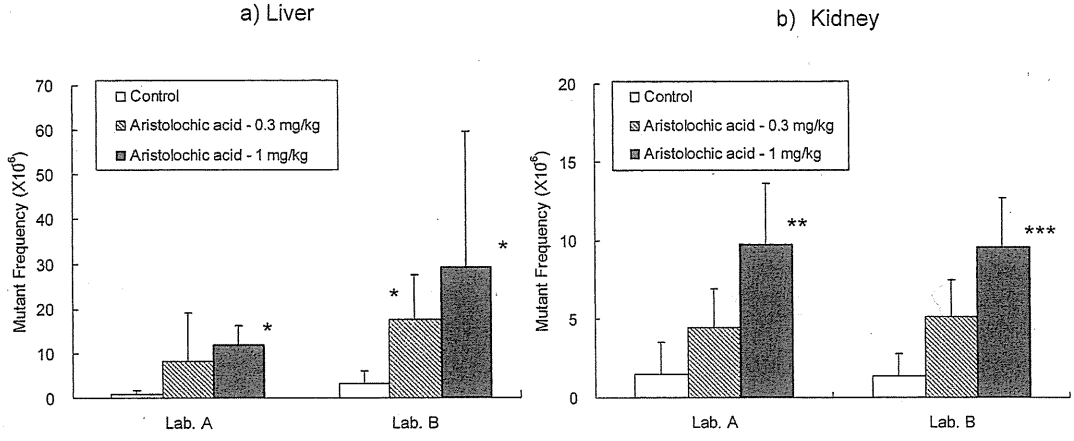

Fig. 1. Comparison between two laboratories in *gpt* mutant frequency of aristolochic acid-treated rats ($n=5$) in a) Liver, b) Kidney. Values represent mean +/−SD. $^{*}p<0.05$, $^{**}p<0.01$, $^{***}p<0.001$ (Steel test).

Table 1. *gpt* Mutant frequencies in the liver of *gpt* delta rats treated with aristolochic acid

Treatment	Animal No.	Total population	Number of mutants	Mutant frequency ($\times 10^{-6}$)	Mutant frequency Average	Mutant frequency SD
Control (Purified water)	1	1,755,000	6	3.42	1.92	1.02
	2	1,158,000	1	0.86		
	3	1,527,000	2	1.31		
	4	654,000	1	1.53		
	5	813,000	2	2.46		
Aristolochic acid (0.3 mg/kg)	11	606,000	5	8.25	12.28***	8.05
	12	729,000	3	4.12		
	13	540,000	10	18.52		
	14	798,000	6	7.52		
	15	261,000	6	22.99		
Aristolochic acid (1 mg/kg)	21	1,107,000	28	25.29	15.29***	6.25
	22	1,149,000	14	12.18		
	23	888,000	15	16.89		
	24	1,104,000	10	9.06		
	25	1,227,000	16	13.04		
N-Ethyl-*N*-nitrosourea (50 mg/kg)	51	336,000	46	136.90	110.16§§§	26.03
	52	447,000	44	98.43		
	53	507,000	54	106.51		
	54	417,000	56	134.29		
	55	576,000	43	74.65		

$^{**}p<0.01$, $^{***}p<0.001$ (Dunnett test), $^{§§§}p<0.001$ (welch's t-test).

Table 2. *gpt* Mutant frequencies in the kidney of *gpt* delta rats treated with aristolochic acid

Treatment	Animal No.	Total population	Number of mutants	Mutant frequency ($\times 10^{-6}$)	Mutant frequency Average	Mutant frequency SD
Control (Purified water)	1	1,020,000	2	1.96	1.69	1.07
	2	921,000	3	3.26		
	3	2,820,000	1	0.35		
	4	1,656,000	2	1.21		
	5	597,000	1	1.68		
Aristolochic acid (0.3 mg/kg)	11	1,254,000	6	4.78	4.82**	1.36
	12	510,000	2	3.92		
	13	669,000	4	5.98		
	14	1,932,000	6	3.11		
	15	474,000	3	6.33		
Aristolochic acid (1 mg/kg)	21	954,000	10	10.48	9.14***	3.60
	22	1,965,000	19	9.67		
	23	1,719,000	9	5.24		
	24	987,000	14	14.18		
	25	1,797,000	11	6.12		

**$p<0.01$, ***$p<0.001$ (Dunnett test).

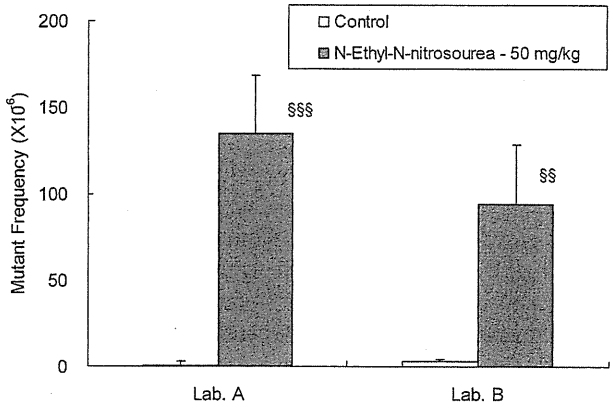

Fig. 2. Comparison between two laboratories in *gpt* mutant frequency of *N*-Ethyl-*N*-nitrosourea-treated rats ($n=5$) in liver. Values represent mean +/−SD. §§$p<0.01$, §§§$p<0.001$ (welch's t-test).

ries generated quite similar results. In the liver, the mean numbers of *gpt* MFs in both Lab. A and Lab. B were 1.92 ± 1.02, 12.28 ± 8.05, and 15.29 ± 6.25 ($\times 10^6$) in the groups treated with 0, 0.3, and 1 mg/kg aristolochic acid, respectively (Table 1). The numbers of *gpt* MFs in the liver in the aristolochic acid treatment groups increased in a dose-dependent manner to approximately 6.4- and 8.0-fold that in the controls, for the 0.3 and 1 mg/kg treatments, respectively. These increases in MFs were statistically significant ($p=0.00054$ and 0.00011, respectively).

In the kidney, the mean numbers of *gpt* MFs in both Lab. A and Lab. B were 1.69 ± 1.07, 4.82 ± 1.36, and 9.14 ± 3.60 ($\times 10^6$) in the groups treated with 0, 0.3, and 1 mg/kg aristolochic acid, respectively (Table 2). The *gpt* MFs in the kidney in the aristolochic acid treatment groups increased in a dose-dependent manner to approximately 2.9- and 5.4-fold that in the controls. These increases in MFs were also statistically significant ($p=0.00843$ and 0.00043, respectively).

In the positive control group treated with 50 mg/kg ENU for 5 days, Lab. A and Lab. B showed very similar *gpt* MF in the liver of rats (Fig. 2). The *gpt* MF in the liver was 110.16 ± 26.03 ($\times 10^6$), which was approximately a 57.4-fold increase compared with the negative control group (Table 1). This increase in MFs was also statistically significant ($p=0.00036$).

Evaluation of the toxicity of aristolochic acid: A summary of the toxicity data generated for aristolochic acid is shown in Table 3. No mortalities occurred at any dose level during the dosing period. In the clinical observation, hematology, autopsy, and measurements of body weights, organ weights, and food intakes, no significant changes related to treatment with aristolochic acid were found at any dose. In the blood chemistry, the ALT value increased very slightly in the 1 mg/kg group. In the histopathology, very slight mononuclear infiltrations of the liver and very slight basophilic tubules in the kidney were observed in both of the 0.3 mg/kg and 1 mg/kg groups.

Discussion

The aim of the present study was to assess the utility of *gpt* delta transgenic rats and the adequacy of the IWGT-recommended general protocol (9) through a genotoxicity risk assessment of aristolochic acid in the kidney and liver of rats. Aristolochic acid was administered orally to *gpt* delta rats at doses of 0.3 and 1 mg/kg for 28 days, and the animals were autopsied 3 days after the last treatment so that the liver and kidney